Geological Society of America Bulletin

Orogenic wedge advance in the northern Andes: Evidence from the Oligocene-Miocene sedimentary record of the Medina Basin, Eastern Cordillera, Colombia

Mauricio Parra, Andrés Mora, Carlos Jaramillo, Manfred R. Strecker, Edward R. Sobel, Luis Quiroz, Milton Rueda and Vladimir Torres

Geological Society of America Bulletin 2009;121;780-800
doi:10.1130/B26257.1

Orogenic wedge advance in the northern Andes: Evidence from the Oligocene-Miocene sedimentary record of the Medina Basin, Eastern Cordillera, Colombia

Mauricio Parra[†]
Andrés Mora[§]
Institut für Geowissenschaften, Universität Potsdam, D-14476 Potsdam, Germany

Carlos Jaramillo
Center for Tropical Paleoecology and Archeology, Smithsonian Tropical Research Institute, Box 0843-03092, Balboa, Panama

Manfred R. Strecker
Edward R. Sobel
Institut für Geowissenschaften, Universität Potsdam, D-14476 Potsdam, Germany

Luis Quiroz
Center for Tropical Paleoecology and Archeology, Smithsonian Tropical Research Institute, Box 0843-03092, Balboa, Panama

Milton Rueda
Vladimir Torres
Instituto Colombiano del Petróleo, Ecopetrol, AA 4185, Bucaramanga, Colombia

ABSTRACT

Foreland basin development in the Andes of central Colombia has been suggested to have started in the Late Cretaceous through tectonic loading of the Central Cordillera. Eastward migration of the Cenozoic orogenic front has also been inferred from the foreland basin record west of the Eastern Cordillera. However, farther east, limited data provided by foreland basin strata and the adjacent Eastern Cordillera complicate any correlation among mountain building, exhumation, and foreland basin sedimentation. In this study, we present new data from the Medina Basin in the eastern foothills of the Eastern Cordillera of Colombia. We report sedimentological data and palynological ages that link an eastward-thinning early Oligocene to early Miocene syntectonic wedge containing rapid facies changes with an episode of fast tectonic subsidence starting at ca. 31 Ma. This record may represent the first evidence of topographic loading generated by slip along the principal basement-bounding thrusts in the Eastern Cordillera to the southwest of the basin. Zircon fission-track ages and paleocurrent analysis reveal the location of these thrust loads and illustrate a time lag between the sedimentary signal of topographic loading and the timing of exhumation (ca. 18 Ma). This lag may reflect the period between the onset of range uplift and significant removal of overburden. Vitrinite reflectance data document northward along-strike propagation of the deformation front and folding of the Oligocene syntectonic wedge. This deformation was coupled with a nonuniform incorporation of the basin into the wedge-top depozone. Thus, our data set constitutes unique evidence for the early growth and propagation of the deformation front in the Eastern Cordillera, which may also improve our understanding of spatiotemporal patterns of foreland evolution in other mountain belts.

Keywords: Andes, Columbia, Cenozoic, inversion tectonics, foreland basin, fold-and-thrust belts.

INTRODUCTION

The stratigraphic record of a foreland basin yields an important archive of the tectonic and climatic evolution of a mountain belt. A close link among shortening, thrust loading, and the flexural response of continental lithosphere, as well as associated changes in topography, is ultimately reflected in the creation of accommodation space for large volumes of sediments (Beaumont, 1981; Jordan, 1981; Flemings and Jordan, 1989; DeCelles and Giles, 1996). As a result, spatiotemporal variations in the magnitude of these parameters can be inferred from trends in the three-dimensional evolution of sedimentary facies and the geometry (i.e., wavelength) of foreland basins (Flemings and Jordan, 1990). For example, observations from many mountain belts and deduced conceptual models of orogenic evolution illustrate that migration of thrust loading and the development of characteristic facies belts are directed toward the foreland (e.g., Sinclair, 1997; DeCelles et al., 1998; Ramos et al., 2002; DeCelles, 2004; Horton, 2005). However, changes in the sense of propagation of the foreland basin depozones may follow changes in the distribution of thrust loading, where out-of-sequence faulting (e.g., DeCelles and Giles, 1996) and deceleration and thickening of the thrust wedge (e.g., Sinclair et al., 1991) promote orogenward migration of the foreland basin depozones. Alternatively, episodic defor-

[†]E-mail: mauricio@geo.uni-potsdam.de
[§]Current Address: Instituto Colombiano del Petróleo, Ecopetrol, AA 4185, Bucaramanga, Colombia

GSA Bulletin; May/June 2009; v. 121; no. 5/6; p. 780–800; doi: 10.1130/B26257.1; 9 figures; 2 tables; Data Repository item 2008215.

mation along a stationary deformation front, reflected in alternating stages of thrust loading and either quiescence or erosional unloading, may account for spatial shifts of the foreland basin depositional environments (Flemings and Jordan, 1990; Catuneanu et al., 1997, 1998). A long-term stagnation of the foreland basin system may also result from lateral variations in flexural rigidity of the flexed plate (Waschbusch and Royden, 1992). Alternatively, its internal structure may be fundamentally influenced by inherited basement inhomogeneities, along which deformation is preferentially accommodated during subsequent orogenic processes (e.g., Hilley et al., 2005). Testing such models in natural settings is thus important and requires a multidisciplinary approach that allows identification of trends in sedimentary facies and subsidence rates in the basin, and of the location of thrust loads through time (e.g., Jordan, 1995).

The Cenozoic Andes constitute one of the best suited settings to closely examine these issues. The Andes orogen is the type example of a retroarc foreland basin (e.g., Jordan, 1995; Ramos et al., 2002). Along different sectors of the southern and central Andes of Argentina and Bolivia, the onset of mountain building during contractional deformation has been widely documented using the architectural characteristics of depositional foreland sequences and provenance data (e.g., Damanti, 1993; Jordan et al., 1993; Coutand et al., 2001; Horton et al., 2001; Dávila and Astini, 2003; Echavarria et al., 2003; Uba et al., 2006). A long-term pattern of cratonward migration of the orogenic wedge leading to the formation of fold-and thrust belts (e.g., Coutand et al., 2001; Ramos et al., 2002; Echavarria et al., 2003) has been explained as the result of deformation acting on a relatively mechanically homogeneous crust, largely controlled by critical Coulomb wedge mechanics (e.g., Horton, 1999; Hilley et al., 2004). However, a nonsystematic pattern of lateral orogenic growth or the absence of typical wedge geometries may occur in those settings, where favorably oriented basement anisotropies in front of an orogenic wedge may absorb shortening. This is apparently the case in the Santa Barbara system and the northern Sierras Pampeanas of NW Argentina, where deformation tends to be accommodated along basement inhomogeneities inherited from previous tectonic events (e.g., Allmendinger et al., 1983; Ramos et al., 2002; Hilley et al., 2005; Mortimer et al., 2007).

In contrast to these morphotectonic provinces of the southern central Andes, in the northern Andes of Colombia, a detailed documentation of foreland basin evolution has thus far only been accomplished in the more internal sectors

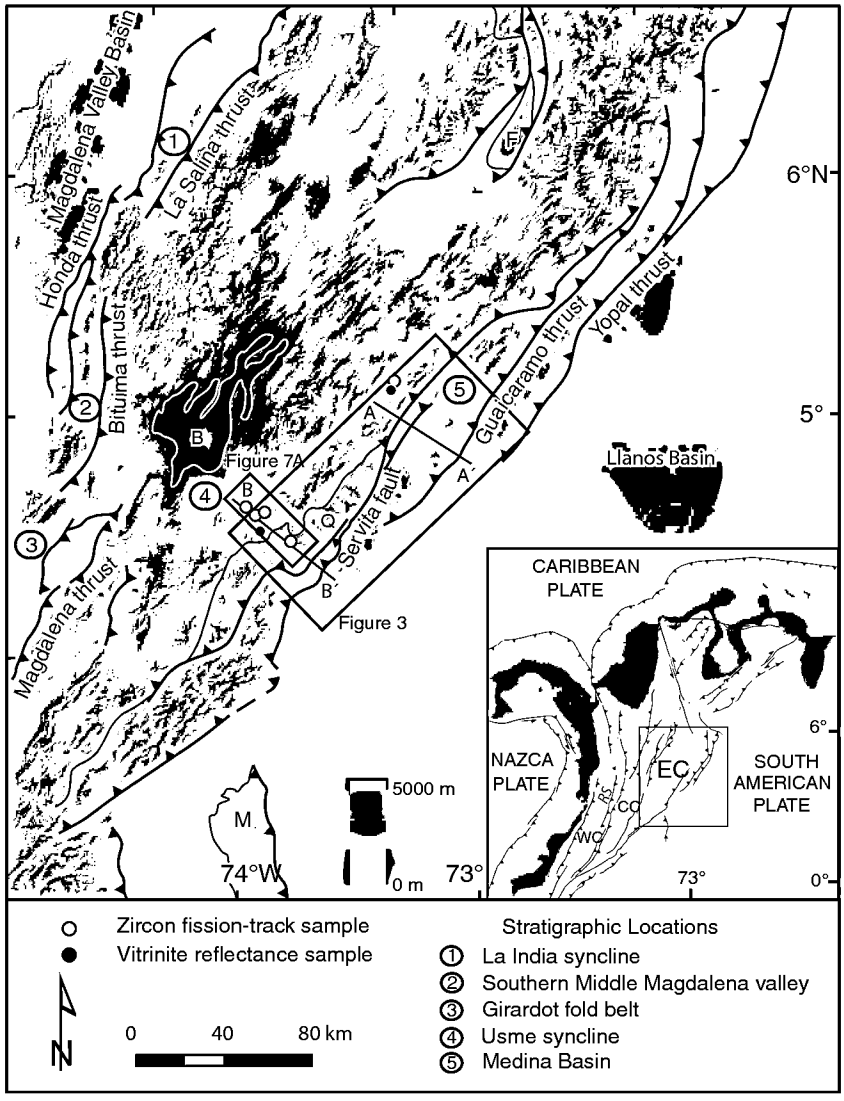

Figure 1. A 90 m STRM (Shuttle Radar Topography Mission) digital elevation model (DEM) showing that the major thrusts delimit topographic breaks in the Eastern Cordillera of Colombia. The black lines mark the boundary of the Floresta (F) and Quetame (Q) basement highs and the Macarena Range (M). The white line shows the extent of the High Plain of Bogotá (B). Locations of vitrinite reflectance and zircon fission-track samples in the area of the Quetame massif are indicated. Stratigraphic locations referred to in the text are shown with numbers 1–5. Inset shows the geodynamic setting of the Western (WC), Central (CC), and Eastern (EC) Cordilleras, and the Romeral Suture (RS) within the northern Andes. The black frame denotes area covered by Figures 3 and 7. Box in inset indicates the location of the main map.

of the orogen (Fig. 1), such as the Central Cordillera and the Magdalena Valley Basin (Cooper et al., 1995; Gómez et al., 2003, 2005; Montes et al., 2005; Ramon and Rosero, 2006). Uplift of the Central Cordillera since the Late Cretaceous and episodic deformation (Gómez et al., 2005) have been inferred to account for the Paleogene facies distribution and basin geometry in this region. Also, an episode of orogenward progression of the foreland basin system has been identified for the early stages of basin development during the late Paleocene (Gómez et al., 2005). Despite these recent improvements in our understanding of foreland development in this part of the Andes, details of the tectonic and stratigraphic expressions of the advance of the orogenic front farther to the east remain ambiguous and largely unidentified. Particularly due

to a lack of timing constraints for deformation in the eastern sectors of the Eastern Cordillera, the spatiotemporal evolution of thrust systems, the associated creation of topography, and the chronology of denudation and sedimentation are not very well known in this region. Along both flanks of the Eastern Cordillera, the presence of basement inhomogeneities associated with Mesozoic normal faults reactivated during Cenozoic compressional tectonics (e.g., Mora et al., 2006, 2008b) offers the possibility of assessing their role in the localization of deformation during orogenic evolution.

In this paper, we unravel the early history of mountain building along the eastern border of the Eastern Cordillera of Colombia through analysis of the sedimentary record preserved in the Medina Basin, along the eastern foothills of the range between 4°20′N and 5°00′N latitude. We integrate new detailed geologic mapping of an ~1500 km² area and structural interpretation of ~50 km of two-dimensional (2D) industry-style seismic-reflection profiles with new sedimentologic and biostratigraphic information. We combine these results with new thermal maturation data based on vitrinite reflectance from the foreland basin sediments, and new zircon fission-track (ZFT) ages from bedrock in the hinterland to provide a detailed account of the evolution of the northern Andean orogenic front in central Colombia. This approach helps document the effects of tectonic loading along individual thrust sheets, illustrates along-strike propagation of faulting, and documents the advance of the orogenic front toward the foreland beginning in early Oligocene time. Collectively, our new data allow a more robust evaluation of the different mechanisms influencing the development of the Colombian foreland system through time.

TECTONIC SETTING AND GEOLOGICAL BACKGROUND

The Colombian Andes consist of three principal, northeast-southwest–oriented geologic provinces (Fig. 1): (1) an allochthonous sector of accreted oceanic paleo-Pacific crust west of the Romeral suture, which constitutes the Western Cordillera and the Baudo Range; (2) a central zone, defined by Proterozoic continental basement covered by upper Paleozoic platformal sequences, rift-related Mesozoic sediments, and Cenozoic marine and nonmarine sedimentary rocks, which underwent significant Cenozoic shortening and now constitutes the Central and Eastern Cordilleras and the intermontane Magdalena Valley Basin; and (3) the Guyana Shield province to the east, where crystalline Proterozoic basement, lower to upper Paleozoic, Mesozoic (post-Cenomanian), and Cenozoic strata occur below a veneer of Quaternary sediments (e.g., Cooper et al., 1995).

East of the Central Cordillera, a foreland basin system has evolved in response to shortening and uplift of this range since the Late Cretaceous (Cooper et al., 1995; Gómez et al., 2003). Oblique accretion of oceanic rocks in the Western Cordillera (McCourt et al., 1984) has been suggested as the driving mechanism for the Late Cretaceous initiation of uplift, loading, and foreland basin development (Cooper et al., 1995). In contrast, the Eastern Cordillera is a north-northeast–oriented bivergent inversion orogen related to Cenozoic reactivation of Cretaceous rift structures during E-W–oriented compression (Colletta et al., 1990; Cooper et al., 1995; Mora et al., 2006). The Eastern Cordillera constitutes the eastern limit of the Colombian Andes, abutting the virtually undeformed lowlands of the Llanos Basin (Fig. 1). Tectonic inversion has compartmentalized a once-contiguous foreland province, including areas east of the Central Cordillera, the present-day intermontane Magdalena Valley Basin, and the Llanos Basin to the east. The principal phase of tectonic inversion in the Eastern Cordillera is thought to have started in the Miocene (Van der Hammen, 1958; Cooper et al., 1995) and has been attributed to the collision of the Baudó-Panama arc with the western active margin of South America (Duque-Caro, 1990). The appearance of post–middle Miocene alluvial sediments in the Llanos Basin has been linked to the onset of uplift and exhumation in the Eastern Cordillera (Van der Hammen, 1958; Dengo and Covey, 1993; Cooper et al., 1995). Direct indicators of Cenozoic deformation in the Eastern Cordillera are known from the western and, to a lesser extent, central and northeastern parts of the mountain range. To the west, in the middle Magdalena Valley Basin (La India syncline, number 1 in Fig. 1), middle Eocene strata rest unconformably over folded early Paleocene units associated with west-verging thrust sheets. This constrains an episode of late Paleocene to early Oligocene deformation (Restrepo-Pace et al., 2004). Approximately 120 km to the south (number 2 in Fig. 1), middle Eocene to Oligocene nonmarine growth strata associated with west-verging, thrust-related folding (Gómez et al., 2003) document initial deformation of the Eastern Cordillera. Farther to the south (number 3 in Fig. 1), the local unconformable relationship between upper Cretaceous and Oligocene-Miocene deposits in the Girardot fold belt (e.g., Raasveldt, 1956; Montes et al., 2005) has been interpreted to reflect pre-Oligocene to Miocene erosion as a response to folding along the western flank of the Eastern Cordillera (Gómez et al., 2003; Montes et al., 2005). In the axial part of the Eastern Cordillera, the structural configuration of an upper Cretaceous to Oligocene sedimentary sequence from the eastern flank of the Usme syncline (Julivert, 1963; number 4 in Fig. 1) has been interpreted as growth strata related to folding and the resultant creation of subdued topography (Gómez et al., 2005). Finally, along the northeastern margin of the Eastern Cordillera, subsurface data have been used to infer late Eocene to late Oligocene thin-skinned deformation (Corredor, 2003; Martínez, 2006). However, the surficial sedimentological and structural expression of this inferred deformation episode remains ambiguous. Furthermore, the exact timing of initial deformation and spatiotemporal variations along strike is still poorly resolved.

Despite these problems and limitations, integrated regional reconstructions and geodynamic modeling have attempted to constrain the onset of mountain building in the Eastern Cordillera. Despite evidence for a pre–middle Miocene onset of thrust loading, the inferred timing and locus of thrusting differ significantly among these models. For instance, at ~4.5°N latitude, tectonic loading in the present-day axial sector of the mountain range has been inferred to have started in the Late Cretaceous (Bayona et al., 2006; Ojeda et al., 2006). Conversely, Sarmiento-Rojas (2001) suggested initial loading during the late Paleocene in the eastern foothills region. Here, a minor contribution of remaining thermal subsidence inherited from Mesozoic rifting was also suggested for the late Paleocene by this author. Finally, Gómez et al. (2005) modeled loading along the axial Eastern Cordillera as having started in the late Eocene–early Oligocene. These temporal disparities in the initiation of loading along the Eastern Cordillera call for a direct assessment of the tectono-sedimentary evolution of the range and the adjacent basins, involving the integration of the uplift history of the hinterland with an analysis of the response of the basin with respect to crustal thickening and exhumation.

The record of foreland basin evolution is preserved in the Late Cretaceous to Holocene deposits east of the Central Cordillera. These strata consist of an up to 7-km-thick succession evolving from estuarine and coastal-plain to proximal fluvial deposits (Gómez et al., 2003). Cenozoic uplift of the Eastern Cordillera caused either erosional removal or nondeposition in this part of the succession. Consequently, an incomplete record of foreland basin sedimentation is preserved in the internal sectors of the mountain range and is exposed mainly along syncline inliers. In the area surrounding the High Plain of Bogotá, for example, upper Miocene alluvial deposits (Tilatá and Marichuela Formations; Helmens and Van der Hammen,

1994) rest unconformably on middle Eocene to lower Oligocene nonmarine sediments (Usme and Regadera Formations; Hoorn et al., 1987; Kammer, 2003; Gómez et al., 2005; Fig. 2). In contrast, a complete record of Cenozoic sedimentation is exposed in elongated basins along fold-and-thrust belts on either side of the Eastern Cordillera (e.g., Cooper et al., 1995). Along the eastern margin of the range at 4.5–5°N latitude, the Medina Basin is particularly well suited for determining the initial stages of orogenesis in this part of the Andes (Fig. 1). First, it is located within the present-day wedge-top depozone of the foreland basin system between the deeply exhumed basement high of the Quetame massif to the west and the presently deforming mountain front demarcated by the Guaicaramo thrust to the east. Second, ~5 km of shallow-marine and nonmarine syntectonic sediments (Fig. 2) are well exposed and preserved within the fold-and-thrust belt and thus offer an unrestricted view of Cenozoic orogenic processes.

METHODS

The apparent discrepancies in the early spatiotemporal localization of the leading edge of deformation in the Eastern Cordillera led us to employ a multidisciplinary approach aimed at linking the uplift and exhumation in the Quetame massif with the creation of accommodation space and the depositional history in the adjacent Medina Basin. In order to identify variations in thickness and lithology within laterally equivalent lithostratigraphic units across the Medina Basin, we mapped an area of ~1500 m^2 at a scale of 1:10,000. Field observations were integrated with the interpretation of two-dimensional industry-style seismic-reflection profiles to better document the lateral continuity and geometry of sedimentary units. We analyzed stratigraphic sections and facies along three sections to document lithofacies variations at different positions within the basin. Approximately 180 measurements of paleocurrent indicators (e.g., DeCelles et al., 1983) were carried out to reveal patterns of sediment dispersal. To better constrain the depositional history, we provide a new palynological biozonation based on analysis of 125 samples. We identified 169 palynomorph species and counted a total of

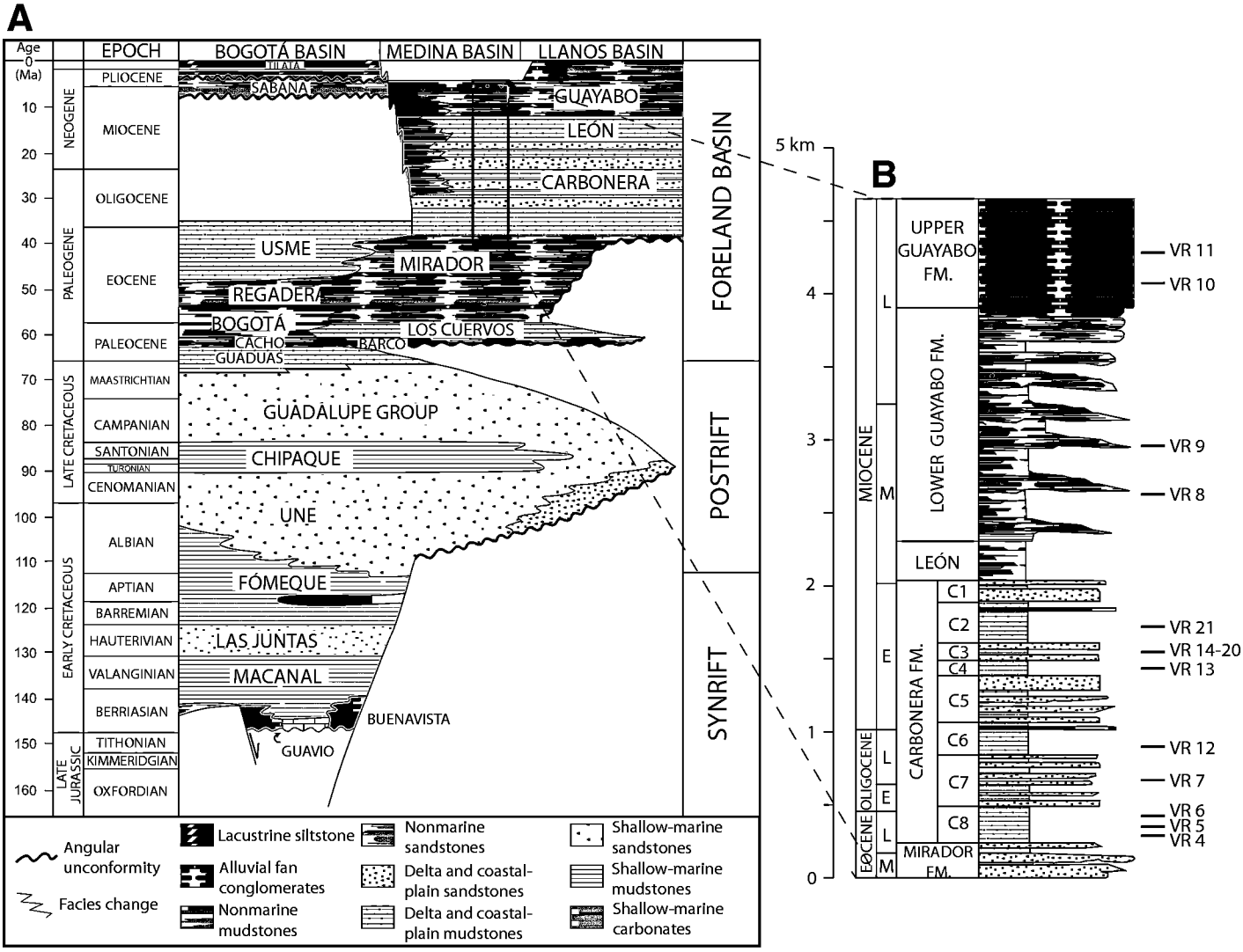

Figure 2. (A) Generalized stratigraphy of the eastern margin of the Eastern Cordillera and the Llanos Basin showing the spatiotemporal distribution of Cretaceous rift-related and Cenozoic foreland basin sedimentary units. (B) The Upper Eocene–Miocene stratigraphy of the Medina Basin consists of an ~4.5-km-thick, first-order, coarsening-upward succession. Locations of samples for vitrinite reflectance analyses are indicated.

16,379 grains (Tables DR1–DR4[1]). All samples were collected from unoxidized, organic mudstone beds along stratigraphic profiles 1, 2, and 3 (18, 71, and 36 samples, respectively; Fig. 4). Sample preparation followed standard procedures (Traverse, 1988), further detailed in the GSA Data Repository (see footnote 1).

Our new stratigraphic results were combined with published data in order to investigate the mechanisms and patterns of subsidence in the basin. We performed one-dimensional backstripping following the procedure described by Allen and Allen (2005), aimed at estimating the changing depth of the basin floor through time. Regional changes in accommodation patterns were assessed by comparing our results from the Medina Basin with published data from the Magdalena Valley (Gómez et al., 2005), ~170 km to the west (Fig. 1).

Spatial comparison of the degree of sediment burial across the Medina Basin was conducted through vitrinite reflectance (VR) analysis (e.g., Guidish et al., 1985). Vitrinite reflectance values (Ro) have been shown to correlate with the maximum temperature reached by organic matter–bearing sediments during heating, allowing for burial assessment in basin analysis (e.g., Tissot et al., 1987). We sampled sediments rich in organic matter and coal beds at different stratigraphic levels within the Cenozoic sedimentary units of the Medina Basin and analyzed 26 samples following standard procedures (e.g., Barker and Pawlewicz, 1993, and references therein). Ro values were converted to maximum paleotemperatures using the kinetic model of Burnham and Sweeney (1989) for heating rates of 0.5 and 50 °C/m.y. These values represent maximum temperatures attained during burial and, when evaluated for lateral equivalent units across the basin, allow for spatial comparison of the degree of burial within the basin.

In order to obtain information on the initial exhumation of the Eastern Cordillera in response to Cenozoic Andean uplift, we performed bedrock thermochronology using the high-temperature zircon fission-track (ZFT) system, targeting upper structural levels within lower Cretaceous, synrift shallow-marine rocks from the Quetame massif area. Fission-track thermochronology is based on the accumulation of linear damage zones (i.e., fission tracks) in the crystal lattice of uranium-bearing minerals caused by the spontaneous fission decay of ^{238}U (Wagner and van den Haute, 1992). Fission tracks are unstable and are progressively erased with time and temperature (e.g., Green et al., 1986), and, therefore, they are useful for extracting the thermal history of the rocks containing the analyzed mineral. The range of temperatures at which fission tracks are partially stable constitutes the partial annealing zone (PAZ; e.g., Tagami and O'Sullivan, 2005). The zircon PAZ corresponds to a temperature range of 250 ± 40 °C (e.g., Tagami et al., 1998). Here, we present five ZFT ages obtained from the western flank of the Quetame massif (Fig. 1). Mineral separation and analytical procedures followed conventional methods (e.g., Bernet and Garver, 2005) and are summarized in Table DR5 (see footnote 1).

STRUCTURAL SETTING AND STRATIGRAPHY OF THE EASTERN FOOTHILLS REGION

The Medina Basin is an integral part of the modern wedge-top depozone (DeCelles and Giles, 1996) of the northern Andean foreland basin system. The sedimentary succession of the eastern flank of the Eastern Cordillera encompasses up to 12 km of Mesozoic rift-related and Cenozoic foreland basin deposits that taper eastward onto the pre-Mesozoic basement of the Guyana Shield (Fig. 2). In the following sections, we provide a general background on the structural configuration of the eastern foothills area and the Mesozoic and Cenozoic stratigraphy.

Structural Configuration

The Medina Basin separates the northern termination of the Quetame massif, west of the west-dipping reverse Servitá fault, from the virtually undeformed Llanos plains east of the Guaicaramo thrust (Fig. 1).

The Quetame massif is a basement high, where pre-Devonian phyllitic basement and upper Paleozoic shallow-marine strata are overlain by Cretaceous synrift and postrift deposits (Fig. 2). Contractile deformation in the Quetame massif is thick-skinned and has been mainly accommodated by reactivation of inherited Mesozoic normal faults (e.g., Mora et al., 2006). In this context, the Farallones anticline is a broad hanging-wall fold associated with the tectonic inversion along the Servitá and Lengupá-Tesalia fault systems (Fig. 3). At ~4°50′N latitude, the Farallones anticline plunges northward and displacement along the Tesalia fault decreases. As a result, shortening in the forelimb of the Farallones anticline is accommodated only by folding.

Farther east, the Medina Basin constitutes the hanging wall of a thin-skinned thrust sheet that extends ~40 km east of the Tesalia fault. Here, the Guavio anticline is a broad fault-bend fold related to the Guaicaramo thrust. In the northern part of the basin, west of the Guavio anticline, the Nazareth syncline is a highly asymmetric, east-verging fold that forms the westernmost structure in the area; its western limb is overturned and constitutes the northern extent of the western Medina syncline. The steepening of the western limb of the Medina syncline occurs where the surficial expression of deformation in the western margin of the Quetame massif changes. In the south, deformation at the surface is mainly accommodated by the Servitá fault, whereas in the north, deformation has resulted in fault-propagation folding (Fig. 3).

Finally, southeast of the Guaicaramo thrust, the Llanos Plain constitutes the modern foredeep. Here, deformation is very minor and mainly results from the southward propagation of the Yopal thrust and the associated hanging wall, La Florida anticline, a structure corresponding to a more frontal depocenter within the en echelon segments of the eastern fold-and-thrust belt.

Stratigraphy

The stratigraphy of the eastern flank of the Colombian Eastern Cordillera is composed of three principal subdivisions (Fig. 2): (1) a Lower Cretaceous, shallow-marine sedimentary sequence associated with rifting, up to 5 km thick, is exposed in the internal, elevated areas of the Eastern Cordillera (Mora et al., 2006). These units unconformably overlie either localized backarc Jurassic volcaniclastic sediments (Mojica et al., 1996; Kammer and Sánchez, 2006), an upper Paleozoic shallow-marine sequence, or pre-Devonian phyllites (Campbell and Bürgl, 1965; Mora et al., 2006; Sarmiento-Rojas et al., 2006). (2) Up to 3 km of Upper Cretaceous platformal deposits register the onset of postrift thermal subsidence (Fabre, 1983; Sarmiento-Rojas et al., 2006). (3) Maastrichtian to Recent marginal marine to nonmarine foreland basin–related units reach a thickness of up to ~7 km. These foreland basin units comprise three sedimentary sequences bounded by two major unconformities that merge into a single composite unconformity toward the east (Fig. 2; Cooper et al., 1995; Gómez et al., 2005).

EARLY SYNOROGENIC STRATA OF THE MEDINA BASIN

We present a new stratigraphic framework for the early Eocene to early Miocene foreland

[1]GSA Data Repository Item 2008215, analytical methods and detailed reports for palynological, zircon fission-track, geohistory, and vitrinite reflectance analysis; and outcrop pictures of typical lithofacies., is available at www.geosociety.org/pubs/ft2008.htm. Requests may also be sent to editing@geosociety.org.

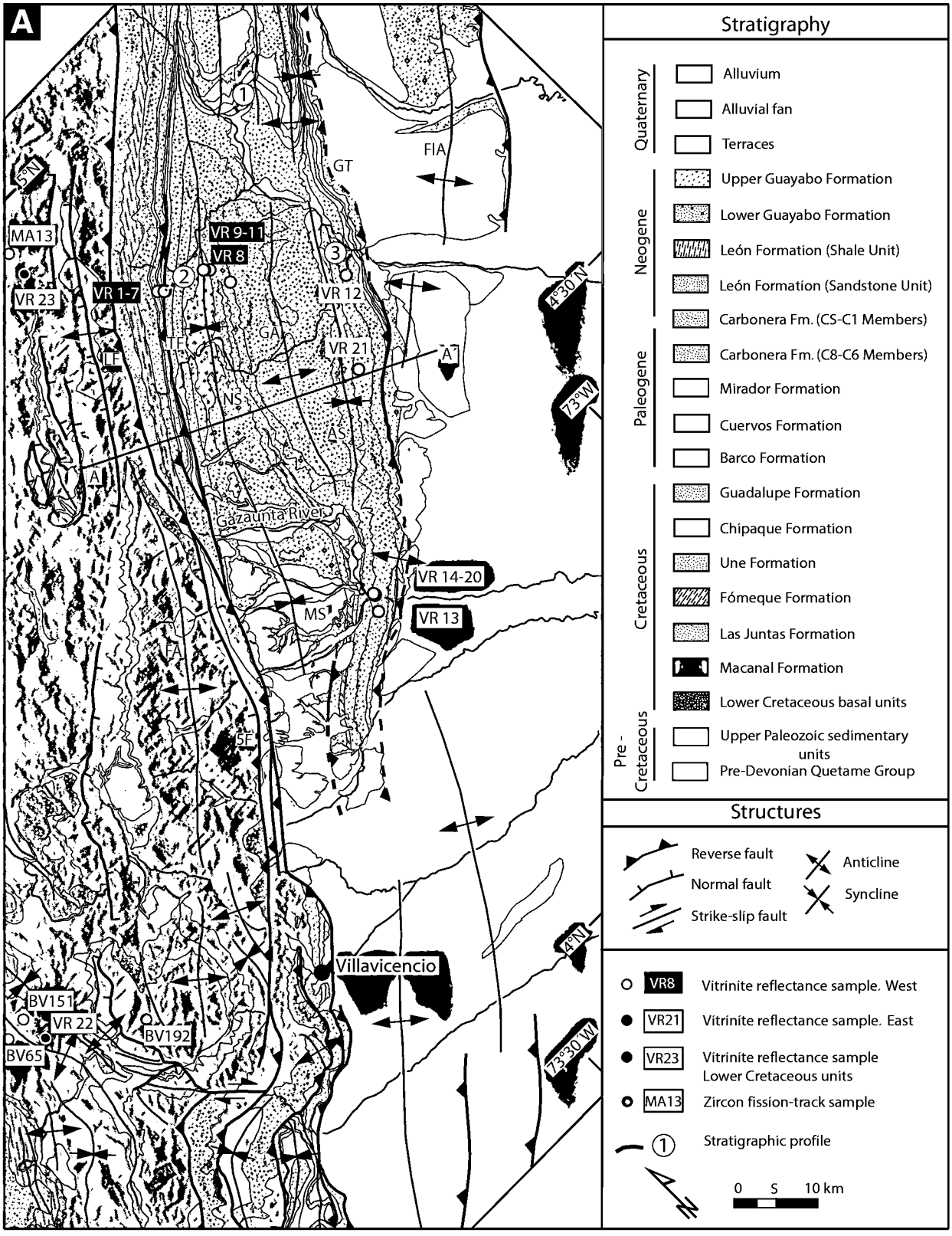

Figure 3. Geological map and cross section of the Medina Basin and the northern termination of the Quetame massif (location shown in Fig. 1). (A) Map depicting main stratigraphic units and structures. Locations of three stratigraphic profiles and sampling sites for zircon fission-track and vitrinite reflectance analyses are indicated. Abbreviations are as follows: AS—Río Amarillo syncline; FA—Farallones anticline; FlA—La Florida anticline; GA—Guavio anticline; GT—Guaicaramo thrust; LF—Lengupá fault; MS—Medina syncline; NS—Nazareth syncline; SF—Servitá fault; TF—Tesalia fault. (*Continued on following page.*)

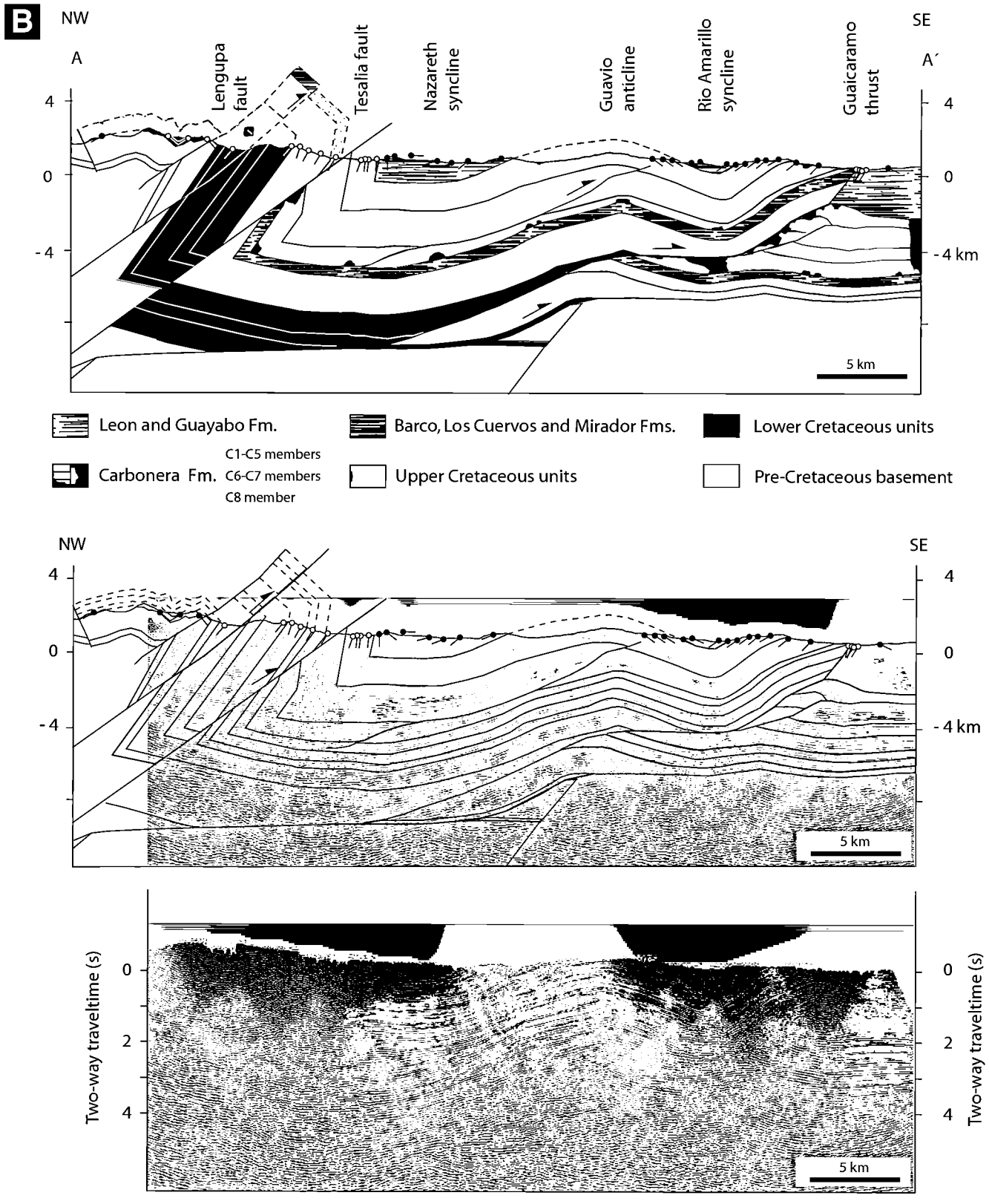

Figure 3 (*continued*). Geological map and cross section of the Medina Basin and the northern termination of the Quetame massif (location shown in Fig. 1). (B) Balanced cross section along structural profile A–A′ (location indicated in A) based on detailed surface mapping and interpretation of seismic-reflection profiles. An eastward-thinning sedimentary wedge made up of the Carbonera Formation is shown.

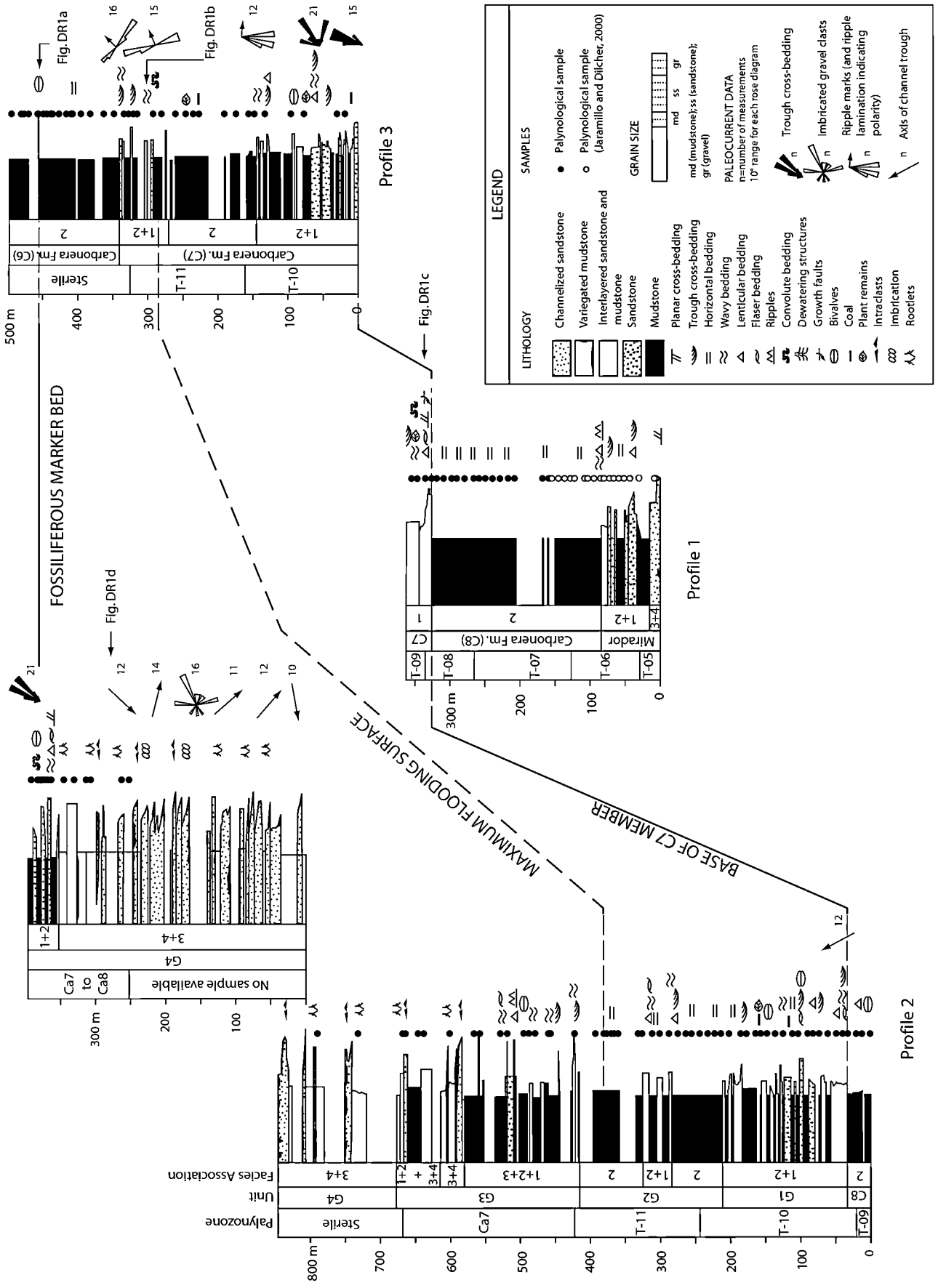

Figure 4. Measured stratigraphic profiles of the C8–C6 members of the Carbonera Formation in the Medina Basin (location in Fig. 3A), including lithostratigraphic correlations, interpreted facies associations, palynological zonations, and paleocurrent measurements. A southwesterly sourced, eastward-thinning clastic wedge corresponding to the C7–C6 members is identified based on lithostratigraphic correlation along distinct marker horizons. Thickness between the base of the C7 member of the Carbonera Formation and a fossiliferous, bivalve-rich marker bed at the top of the C6 member diminishes from ~1150 to ~450 m over a distance of ~20 km. See text footnote 1 for Figure DR1.

basin sediments in the Medina Basin. First, we describe the spatial distribution of sedimentary units and their major lithological and thickness variations, based on our surface and subsurface data. Second, we present facies analyses and paleocurrent data from the lower members of the Carbonera Formation along three stratigraphic profiles across the basin (Fig. 4). Third, we present new biostratigraphic data that allow estimation of depositional ages, and finally we integrate the stratigraphic results to better assess basin evolution during the initial stages of orogenesis in the Eastern Cordillera.

Combined surface mapping and seismic interpretation document the presence of an eastward-thinning sedimentary wedge consisting of the C8–C6 members of the Carbonera Formation (Figs. 3B and 4). The thickness of the C8 member in the northern axial portion of the basin reaches ~250 m (profile 1; Fig. 4). Seismic interpretation tied to detailed geological mapping suggests rapid thickening of this unit to the west (Fig. 3). A varying stratigraphy within the interval delineated by the base of the sandstone-dominated C7 member and a bivalve-rich horizon found at the top of the C6 member across the basin is illustrated based on description along profiles 2 and 3, where a complete record of the C7 and C6 members is described (Fig. 4). Due to lithological variations, we subdivided the equivalent interval into units G1, G2, G3, and G4 in the western profile (Fig. 4). These sections were also sampled for palynology in order to constrain depositional ages and environments. In the following section, we present the facies analysis for the profiled sections.

Depositional Systems

Based on lithology and sedimentary structures, 15 lithofacies (Table 1) and four facies associations were recognized within the C8, C7, and C6 members of the Carbonera Formation. A summary of the facies analysis and the spatial distribution of the facies associations is presented in Table 2 and Figure 4.

Our results show a reversal of paleocurrents from initially westward transport directions in the Mirador Formation, associated with eastern sources on the Guyana Shield (Cooper et al., 1995; Cazier et al., 1997), to a northeastward sediment dispersal pattern. The switch occurs in the C7 and C6 members in the northern and eastern parts of the basin (Fig. 4). This reversal thus documents a change in the main sediment source to the southwest, along the present-day Eastern Cordillera. Limited paleocurrent indicators in the alluvial G4 unit of the western section suggest a polymodal dispersion pattern (Fig. 4), interpreted to reflect episodes of avulsion in the alluvial system.

Our analysis and lithostratigraphic correlation indicate that the C8–C6 Members constitute an eastward-thinning syntectonic wedge in the Medina Basin. In the western part, the interval equivalent to the C7–C6 members reaches a thickness of 1150 m. It evolves from coastal-plain and deltaic deposits in units G1–G3 (facies associations 1 and 2; Table 2) to braided fluvial deposits in unit G4 (facies associations 3 and 4). Equivalent deposits ~20 km to the east are only 455 m thick and are exclusively dominated by deltaic facies associations 1 and 2. Taken together, the rapid facies changes from tidally influenced coastal-plain to fluvial deposits to the west, and the changeover to northeastward paleocurrent directions, document the initial existence of elevated topography in the area of the present-day Eastern Cordillera in early Oligocene time. Furthermore, the thickness variations in the basin clearly illustrate enhanced subsidence in the west, suggesting tectonic loading in the location of the present-day Eastern Cordillera during the late Eocene–late Oligocene.

Age Constraints

Our new chronostratigraphic framework for the C8–C6 members of the Carbonera Formation, based on palynomorphs, facilitates the evaluation of spatiotemporal trends in basin evolution. In our analysis, we follow the biostratigraphic zonal scheme developed by Jaramillo and Rueda (2004), Jaramillo et al. (2005), and Jaramillo et al. (2008). Palynological biozones from northern South America have been calibrated using foraminifera and nanoplankton from Venezuela (Germeraad et al., 1968; Muller et al., 1987) and stable carbon isotopes ($\delta^{13}C$) from Colombia and Venezuela (Jaramillo et al., 2006, 2007). The calibration data provided by these authors suggest that uncertainties in the time assignments of the individual biozones are relatively minor, although the published data are insufficient to further quantify the uncertainty.

Both the eastern and western intervals of the syntectonic wedge corresponding to the C8–C6 members of the Carbonera Formation were deposited within the palynological zones T-05 to Ca-07, corresponding to early Eocene to early Miocene time (Fig. 5). Based on the key taxa for the zonal scheme (Fig. 5), the limits of the biozones in the composite section are assigned to the midpoint between samples belonging to contiguous biozones (Table DR6, see footnote 1). The base of the early Eocene zone T-05 is defined by the first appearance datum (FAD) of *Tetracolporites maculosus*. The FAD of *Cicatricosisporites dorogensis* defines the top of the early Eocene zone T-05. The last appearance datum (LAD) of *Spinizonocolpites grandis* defines the top of the middle Eocene zone T-06. The top of the late Eocene zone T-07 is marked by the LAD of *Echitriporites trianguliformis orbicularis*. The top of the early Oligocene zone T-08 is defined by the LAD of *Nothofagidites huertasii*. The FAD of combined acme of *Jandufouria seamrogiformis*, *Magnastriatites grandiosus*,

TABLE 1. DESCRIPTION AND INTERPRETATION OF LITHOFACIES (AFTER MIALL,1996; EINSELE, 2000)

Code	Description	Interpretation
Gcd	Disorganized clast-supported conglomerates, cobbles, and pebbles	Clast-rich noncohesive debris flow
Gco	Organized, clast-supported conglomerates, cobbles, and pebbles. Weak imbrication	Longitudinal bed forms, lag deposits
St	Trough cross-stratified sandstone, fine to coarse	3D dunes
Sp	Planar cross-stratified sandstone, fine to very coarse, often pebbly	Transverse and linguoid bed forms (2D dunes)
Sr	Ripple marks and small-scale cross-stratification	Ripples (lower flow regime)
Sf	Flaser bedded sandstone	Alternating suspension settling and lower-flow regime
Sw	Wavy bedded sandstone	Alternating suspension settling and lower-flow regime
Slc	Lenticular bedded sandstone	Alternating suspension settling and lower-flow regime
Sc	Convoluted bedded sandstone	Deformation by differential loading or dewatering
Sm	Massive sandstone	Sediment gravity-flow deposits
Fl	Laminated mudstone and siltstone	Suspension-load deposits
Fm	Massive mudstone and siltstone	Suspension deposits, overbank or abandoned channels
Fs	Disorganized shell-dominated mudstone	Upper flow regime
Fb	Variegated mudstone and siltstone. Commonly sandy, intense mottling	Overbank or abandoned channels
Fo	Mudstone and siltstone with organic matter–rich laminae	Suspension settling deposits
C	Coal	Organic-rich swamp deposits

Mauritiidites franciscoi minutus, and *Verrucatosporites usmensis* defines the top of the early to middle Oligocene zone T-09. The LAD of the combined acme of *Jandufouria seamrogiformis*, *Magnastriatites grandiosus*, *Mauritiidites franciscoi minutus*, and *Verrucatosporites usmensis* defines the top of the middle Oligocene zone T-10. The top of the late Oligocene zone T-11 is defined by the LAD of *Cicatricosisporites dorogensis*. Finally, the FAD of *Echitricolporites maristellae* defines the top of zone Ca-07, corresponding to the early Miocene.

GEOHISTORY ANALYSIS

The Paleocene–early Miocene tectonic subsidence history of the Medina Basin was assessed using one-dimensional backstripping of a composite stratigraphic section from the Medina Vasin constructed using the stratigraphic data presented in this study for the lower part of the Carbonera Formation (profiles 1 and 2; Fig. 4), and published data from Paleogene foreland sediments in the basin (Jaramillo and Dilcher, 2000, 2001; see Figs. 4 and 5). Here, we used thicknesses and age constraints for biostratigraphic units based on the palynological biozonation for the Paleocene–early Miocene composite section. Vertical error bars were defined by the stratigraphic separation between the younger and older samples of contiguous biozones. Water-depth estimates were assigned according to the interpreted depositional environments of coastal-plain deposits (see methods in GSA Data Repository [see footnote 1]). Since constraints on Paleogene and Neogene paleoelevations are poor, we assumed a maximum altitude of 300 m, which corresponds to the present maximum altitude of the Llanos Basin alluvial plain. The early to late Miocene sediments of the Upper Carbonera, the León, and Guayabo Formations were treated as a single unit for the analysis. Global long-term eustatic sea-level values (Haq et al., 1987) were averaged over the time span represented by each biostratigraphic unit. A summary of the different parameters used in the geohistory analysis is presented in Table DR6 (see footnote 1).

In order to evaluate the spatial and temporal variations in the subsidence pattern of the foreland basin system, we also plotted an early Paleocene–middle Miocene backstripped section from the southern Middle Magdalena Valley Basin using published data (Gómez et al., 2005). Although geohistory analysis is a powerful method for identifying the components of subsidence, it entails important assumptions that must be taken into consideration when interpreting trends in subsidence patterns.

TABLE 2. SUMMARY OF FACIES ASSOCIATIONS

Facies association	Description	Stratigraphic occurrence (see Fig. 4)	Interpretation
FA1 (coarsening-upward laminated sandstone)	Up to 8-m-thick thickening- and coarsening-upward intervals of tabular sandstone with minor thin interbeds of mudstone. Sandstone beds present nonerosive basal contacts and are frequently bioturbated. Laminae rich in organic matter, plant remains. Thin pebble conglomerate commonly caps intervals at top. Typical lithofacies pattern includes, from base to top, Fm, Fl, Sw, Sf, Slc, Sr, and Gco (see Table 1). Dewatering structures, convolute bedding, and growth faults (Figs. DR1b and DR1c [see text footnote 1]) occur. Sandstone-mudstone couplets with wavy (Sw), lenticular (Slc), flaser (Sf), and oscillatory current ripple lamination (Sr) occur.	In upper 70 m of Mirador Formation (profile 1), in the G1, G2, G3, and uppermost 40 m of G4 units of the Carbonera Formation in the western part of the basin (profile 2), and in C7 member of the eastern section (profile 3).	Thickening- and coarsening-upward intervals suggest progradational succession in a tidally influenced deltaic environment (e.g., Tye and Coleman, 1989; Coleman et al., 1998). Growth faults (Fig. DR1 [see text footnote 1]), convolute bedding, and water-escape structures suggest rapid accumulation (Lowe, 1975; Owen, 1996). Possible allogenic control.
FA2 (massive and laminated dark mudstone)	Thick intervals (up to 100 m) of dark-gray to greenish mudstone. Occasional minor bioturbation. Limited interbeds of trough cross-laminated sandstone, and up to 30-cm-thick coal seams. Occasional thin, disorganized bivalve-bearing shell beds. Local microforaminiferal linings and dinoflagellates. Fragmented and disarticulated bivalves belonging to the genus *Pachydon* (CORBULIDAE; Fig. DR1a [see text footnote 1]). Best preserved specimens resemble the species *P. tenuis*, *P. trigonalis*, and *P. cuneatus*. Discrete levels with microforaminiferal linings and dinoflagellates including *Homotryblium floripes*, *Cordosphaeridium inodes*, *Polysphaeridium subtile*, *Achomosphaera*, *and Spiniferites*.	Dominant facies in C8 and C6 members. Interlayered with FA1 in G1, G2, and G3 units in the western Medina Basin (profile 2).	Mud flat in a deltaic plain. Coal indicates humid climate. Fragmented bivalves belonging to genus *Pachydon* suggest a high-energy, freshwater environment (e.g., Nuttall, 1990; Wesselingh et al., 2002). Dinoflagellates and microforaminiferal linings indicate local marine influence
FA3 (interbedded fluvial sandstones and conglomerates)	Medium- to thick-bedded, medium-to coarse-grained, and pebbly sandstone. Gravel lags and mudstone intraclasts common at base of individual beds. Beds have erosive bases (Fig. DR1d [see text footnote 1]) above mottled sandy mudstones and siltstones, and extend laterally up to few tens of meters. Commonly floating pebble clasts occur. Granule and pebble stringers loosely defining large-scale planar cross-stratification occur rarely. Frequently, strata grade upward into variegated mudstone (FA4).	Occurs in the lower 15 m of measured section of Mirador Formation in profile 1. Occur interlayered with FA4 in G4 unit (western Medina Basin).	Streamflow deposits. Loosely defined large-scale, low-angle planar cross-stratification, absence of well-defined normal grading, and frequent floating pebbles suggest deposition in braided fluvial channels.
FA4 (overbank fines)	Reddish to brown, massive to crudely stratified sandy mudstone and siltstone. Ubiquitous mottling and root traces (Fig. DR1d [see text footnote 1]). Lenticular, normally graded, thin sandstone interbeds.	Major facies of G4 unit. Also in the lower part of Mirador Formation, subordinate to FA3.	Laterally continuous variegated mudstone with pervasive mottling and root traces indicate deposition in an alluvial-plain environment.

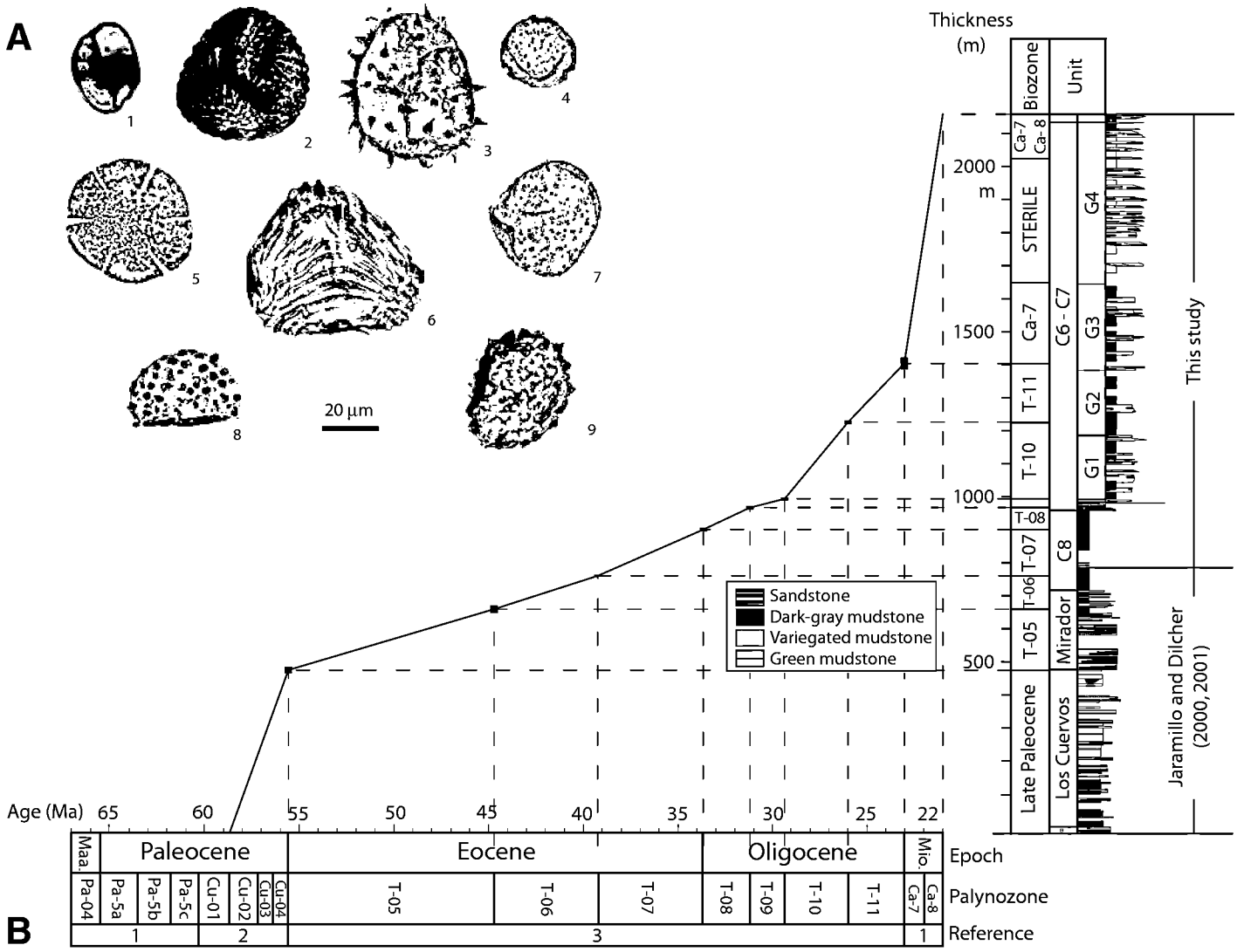

Figure 5. Palynological biozonation and composite stratigraphic section for the upper Paleocene–lower Miocene strata of the Medina Basin. (A) Photographs of key taxa used in this study. 1—*Tetracolporites maculosus*; 2—*Cicatricosisporites dorogensis*; 3—*Spinizonocolpites grandis*; 4—*Echitriporites trianguliformis orbicularis*; 5—*Jandufouria seamrogiformis*; 6—*Magnastriatites grandiosus*; 7—*Mauritiidites franciscoi minutus*; 8—*Verrucatosporites usmensis*; 9—*Echitricolporites maristellae*. See explanation in text. (B). Composite stratigraphic section for the Paleogene strata of the Medina Basin. The composite section is constructed based on thickness, lithology, and biozonation after Jaramillo and Dilcher (2000) for the Los Cuervos and Mirador Formations, and data obtained in this study from profiles 1 and 2 of the Carbonera Formation. The biozonal scheme utilizes the geological time scale of Gradstein et al. (2004). Assignment of biozones is based on Jaramillo and Rueda (2004); and Jaramillo et al. (2005; 2008) (references are coded in zonal scheme with numbers 1, 2, and 3, respectively).

Specifically, local (Airy) compensation of the sediment load neglects lateral flexural strength of the lithosphere and hence results in overestimation of the contribution of the weight of the sediment column to the subsidence of the basin (Watts et al., 1982). Furthermore, in our analysis (Fig. 6) we do not extract subsidence rates, since backstripping only the Cenozoic strata implies that underlying units underwent no compaction during the Cenozoic. Since the pre-Cenozoic substratum in both the Medina and southern Middle Magdalena Valley Basins makes up ~6–7 km of Mesozoic sedimentary rocks (Gómez et al., 2005; Mora et al., 2008a), the total Cenozoic decompacted thickness is overestimated. Consequently, the decompaction curves (Figs. 6A and 6B) are forced to meet the compacted-thickness curves at our time zero (Angevine et al., 1993). Nevertheless, our geohistory analysis is sufficient to allow for comparisons between the western and eastern foothills sections, as we applied the same procedure to a corresponding time interval in both areas.

The Paleocene-Miocene subsidence curves for the Medina and southern Middle Magdalena Valley Basins (Fig. 6) furnish a means to evaluate and compare regional accommodation patterns across the entire foreland basin system. The total subsidence signal for both areas (lowest curves in Figs. 6A and 6B) displays a similar sigmoidal pattern resulting from a period of reduced subsidence (or even uplift in the case of the southern Middle Magdalena Valley, as suggested by the regional Late Cretaceous–Cenozoic unconformity) that separates two episodes with higher accommodation rates. Importantly, the curve for the Medina Basin suggests (1) that the onset of faster subsidence occurred at ca. 31 Ma, at least 30 m.y. after an equivalent episode in the southern Middle Magdalena Valley, and (2) that this episode, starting in the early Oligocene, was responsible for most of the basin subsidence, ultimately leading to a larger amount of total Cenozoic subsidence in the Medina Basin compared to the Magdalena Valley (Fig. 6C). The analysis for the Medina and southern Middle Magdalena Valley Basins shows that the contribution of the sedimentary load to the total subsidence increases through time (Fig. 6C). Since middle Miocene time (ca. 12 Ma), sedimentary loads have accounted for ~70% of the total subsidence in both areas (Fig. 6C). As cautioned earlier, this result is an overestimation due to the simplification introduced by using local (Airy) isostatic compensation. However, the results indicate a different temporal evolution for the sedimentary-load contribution for each area. Mimicking the pattern of the total subsidence curve, the sediment-load contribution in the Medina Basin was minor in the early stages of the foreland basin development. Since early Oligocene time, sedimentary loads have increased until their contribution to the total subsidence reached a similar amount (~70%) compared to the backstripped foreland strata in the Magdalena Valley.

Larger amounts of total and normalized sediment-load–driven subsidence during the Paleocene–early Oligocene (between 65 and 31 Ma; Fig. 6C) in the Middle Magdalena Valley Basin relative to the Medina Basin are compatible with a basin located closer to the orogenic front. Such a basin would have undergone faster subsidence and received a greater load of sediments from the source areas in the hinterland. Maastrichtian to Oligocene tectonic subsidence in the Middle Magdalena Valley Basin has been explained by loading of the Central Cordillera between the Maastrichtian and late Paleocene (Cooper et al., 1995; Gómez et al., 2003, 2005) and by loading of the western front of the Eastern Cordillera in the late Eocene–early Oligocene (Gómez et al., 2003, 2005). The increase in accommodation rates in the Medina Basin since the late Oligocene suggests that the tectonic load, and hence the main source of sediments, has migrated closer to the eastern foothills of the Eastern Cordillera. Despite the limitations of the backstripping method, the analyzed section in the Medina Basin allows us to identify changes in the pattern of tectonic subsidence rates (Fig. 6D). We conclude that the late Paleocene to early Miocene accommodation history in this region is characterized by a three-stage evolution: an initial late Paleocene episode of moderate subsidence; limited subsidence from Eocene through early Oligocene time; and rapid subsidence from early Oligocene through early Miocene time. We correlate the first two stages with a late Paleocene eastward advance, and subsequent Eocene to early Oligocene westward retreat of the foreland basin system. These episodes have also been documented in the foreland basin record of the Magdalena Valley Basin, where they were interpreted as a response to a phase of tectonic activity followed by tectonic quiescence in the Central Cordillera (Gómez et al., 2003, 2005). Similarly, we interpret the second episode of faster tectonic subsidence registered in the late Oligocene–early Miocene sedimentary record of the Medina Basin to result from the eastward advance of the deformation front. Rapid subsidence in the Medina Basin starting at ca. 31 Ma and the concomitant deposition of an eastward-thinning sedimentary wedge are compatible with initial deposition in a foredeep depozone and, hence, are strong evidence for an eastward advance of the orogenic front.

ZIRCON FISSION-TRACK THERMOCHRONOLOGY

Apatite fission-track (AFT) data from in situ bedrock samples from the Quetame massif area show rapid cooling below ~120 °C since ca. 3 Ma and thus reflect fast rock exhumation of 3–5 km since the late Pliocene (Mora et al., 2008a). These data suggest that any older record of exhumation, potentially detectable with AFT, has been erosionally removed from the deeply incised eastern margin of the mountain range. Thus, in order to obtain information on the earlier stages of exhumation, we conducted zircon fission-track (ZFT) analysis. A comprehensive analysis of exhumation patterns is beyond the scope of this paper and will be presented elsewhere. However, although limited, we present data from five samples obtained from the Quetame massif area (Figs. 3 and 7) in order to document the timing of thrust-induced exhumation in this sector of the range. Four samples were collected along a longitudinal profile running across the pre-Devonian to Lower Cretaceous section of the western flank of the Quetame massif. Sampling covered different structural levels in order to determine the limits of the ZFT partial annealing zone in this part of the mountain range. A fifth sample (MA 13) was collected from a similar structural position to that of the uppermost sample (sample BV 121) in the longitudinal profile. However, sample MA 13 was located ~80 km to the northwest along strike. Table DR5 (see footnote 1) shows the individual ages for the five analyzed samples. The three structurally deepest samples pass the χ^2 test (Galbraith, 1981; Green, 1981) with values of $P(\chi^2) > 5\%$ (samples BV 151, BV 192, and MA13), indicating that the single-grain age distribution corresponds to a single component (Fig. 7D). We analyzed the significance of the ZFT cooling ages using an approximation to an age-elevation profile. Age-elevation profiles exploit differences in topographic elevation of samples along relatively steep profiles; if the profile includes part of an exhumed partial annealing zone, it is possible to derive the timing of initiation of exhumation (Wagner and Reimer, 1972; Huntington et al., 2007). In the Quetame massif, the absence of deeply incised canyons cutting through the entire Lower Cretaceous to pre-Devonian section prevents such an approach. Instead, we use detailed structural mapping and a structural cross section (Mora et al., 2006) to project the four samples collected in the southwestern part of the Quetame massif onto a profile. We related the samples to a datum defined by the angular unconformity at the base of the rift-related Cretaceous sedimentary sequence (Fig. 7). The stratigraphic elevation of the samples with respect to this datum was

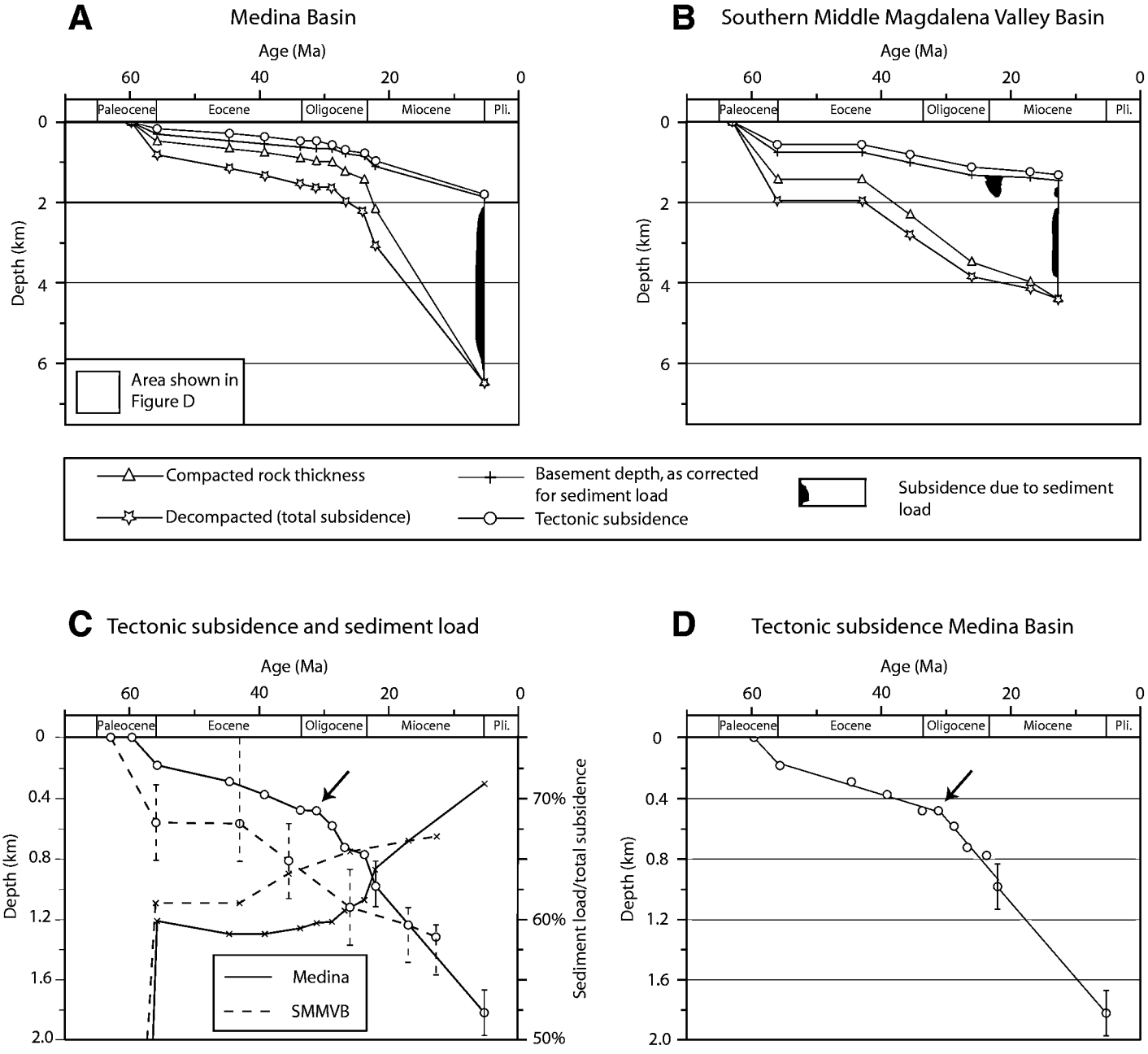

Figure 6. Geohistory analysis for the upper Paleocene–Miocene stratigraphic sections of the Medina and southern Middle Magdalena Valley Basins. (A) Medina Basin. (B) Southern Middle Magdalena Valley Basin (SMMVB) (data from Gómez et al., 2005). Details on parameters used for analyses are shown in Table DR6 (see text footnote 1). (C) Tectonic subsidence curves (black lines) and temporal evolution of the sediment-load contribution to the total (decompacted) subsidence (gray lines) for Medina and southern Middle Magdalena Valley Basins. Rapid subsidence in the southern Middle Magdalena Valley Basin during Paleocene time resulted from tectonic loading of the Central Cordillera (Gómez et al., 2005). Enhanced subsidence since ca. 31 Ma (arrow) in the Medina Basin results from initiation of loading along the present-day eastern border of the Eastern Cordillera. See text for discussion. (D) Tectonic subsidence curve of the Medina Basin depicting a sigmoidal, three-stage pattern interpreted as the vertical stacking of distal foredeep, forebulge, and proximal foredeep, resulting from the Eocene retreat and subsequent Oligocene advance of the foreland basin system. Vertical error bars represent uncertainties in paleoaltitude (water depth) for continental (marine) units. Bars are only visible for the two youngest points representing continental deposits with larger uncertainty in paleoelevation (see Table DR6 [see text footnote 1] and text for discussion).

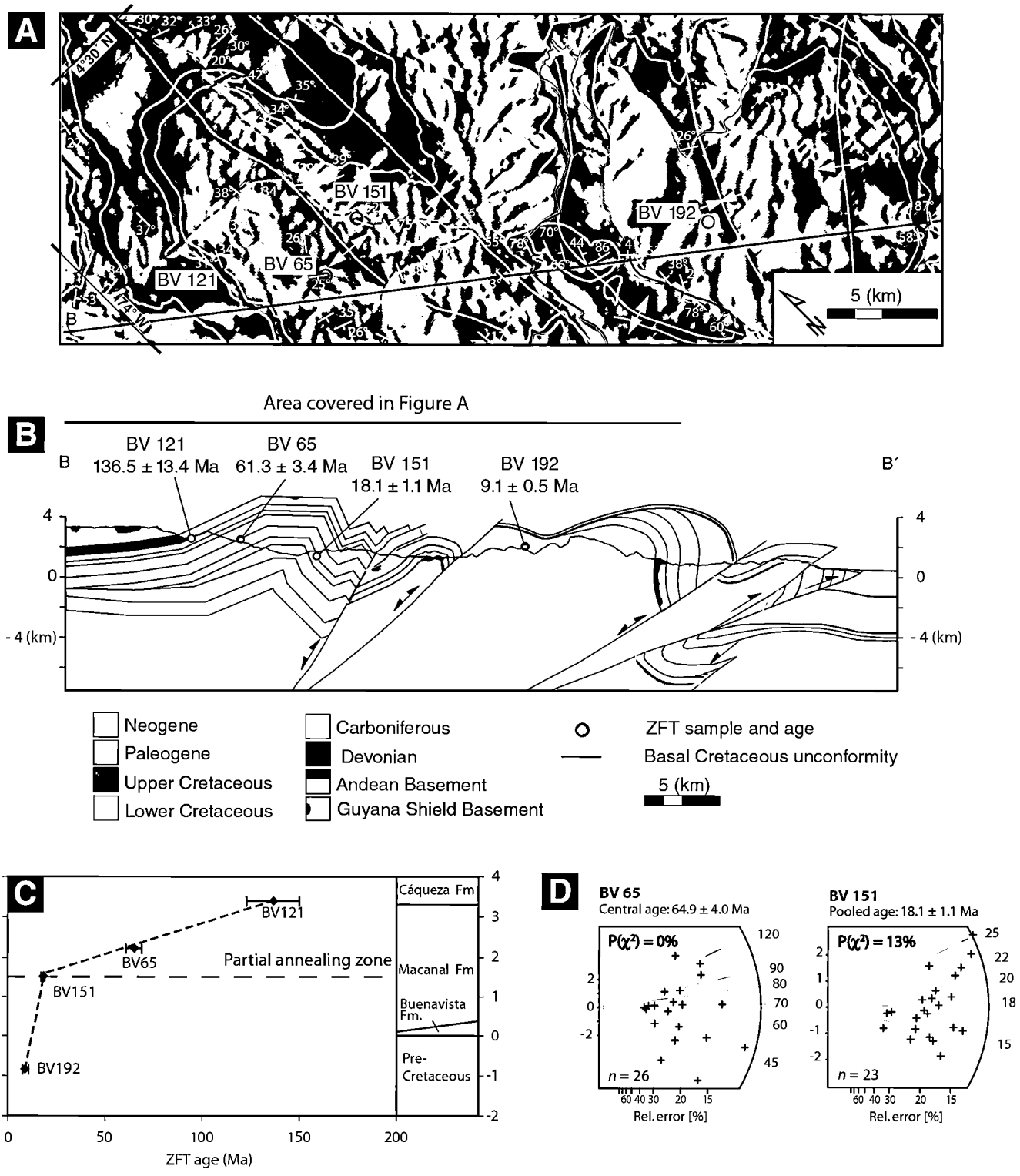

Figure 7. Zircon-fission track (ZFT) data. (A) Geologic map and (B) structural cross section along profile B–B′ (see location also in Fig. 1) illustrating the location of zircon fission-track samples (red dots) and the unconformity at the base of the Lower Cretaceous sedimentary units (blue line; modified from Mora et al., 2006). (C) Structural elevation vs. age profile for the analyzed samples. The upper part of the Macanal Formation, between samples BV 65 and BV 151, delimits the base of an exhumed partial annealing zone. (D) Radial plots for two samples from the Lower Cretaceous rift-related deposits of the Macanal Formation in the Quetame massif. Sample BV 151 passes the chi-squared test ($P[\chi^2] > 5\%$; see Galbraith, 1981; Green, 1981) and thus represents a single age population. Therefore, the reported pooled age of ca. 18 Ma can be interpreted as reflecting early Miocene, thrust-induced exhumation. Sample BV 65 fails the chi-squared test, reflecting a mixed age population as a result of only partial annealing.

plotted versus the zircon fission-track age. The resulting plot illustrates the approximate position of the base of an exhumed partial annealing zone between sample BV 65 ($P[\chi^2] = 0.0$; central age = 61.3 ± 6.4 Ma) and sample BV 151 ($P[\chi^2] > 5\%$; pooled age = 18.5 ± 1.0 Ma; Table DR5 [see footnote 1]; Fig. 7C). Furthermore, the total annealing for the ZFT system of the Lower Cretaceous section is also supported by vitrinite reflectance (VR) data, constraining the maximum postdepositional paleotemperature of the Lower Cretaceous rift-related rocks. Regional Ro values for the shales of the Macanal Formation along the Eastern Cordillera vary between 3.5% and 5% (e.g., Toro et al., 2004) and represent maximum paleotemperatures >250 °C, according to the standard correlation model (Burnham and Sweeney, 1989). Two VR analyses of samples obtained from the western flank of the Quetame massif (Mora et al., 2008a; location in Fig. 3) yielded results similar to the regional trend (Table DR7 [see footnote 1], samples VR22 and VR23).

Sample MA13, from the northern part of the Quetame massif, adjacent to the Medina Basin, yielded a ZFT age of 17.9 ± 1.0 Ma. This age overlaps within 2σ error with the age of the structurally equivalent sample BV 151 from the south (18.5 ± 1.0 Ma). We interpret these early Miocene ZFT ages to represent cooling ages resulting from thrust-induced exhumation of the Quetame massif. However, these ZFT ages postdate the onset of thrust-related exhumation, likely by a small amount, as this information would only be provided by the structurally uppermost rocks just beneath the zircon partial annealing zone. More precise identification of this limit requires more detailed sampling and, ideally, ZFT investigations along near-vertical profiles. However, our results constrain the stratigraphic interval within the upper part of the Macanal Formation along which future studies should be focused.

Early Miocene exhumation and rock uplift in the Quetame massif area contrast with subsidence in the Medina Basin, a few kilometers to the east. Geohistory analysis of the thick sedimentary wedge corresponding to the C8–C6 members of the Carbonera Formation suggests that enhanced tectonic subsidence in the Medina Basin started in the early Oligocene. Combined, the thermochronological results help to better constrain the position of the deformation front of the orogenic wedge, which by the early Oligocene, coincided with the inverted Servitá fault.

VITRINITE REFLECTANCE

Observed mean vitrinite reflectance (Ro) values in the Paleocene to Miocene sedimentary rocks of the basin vary between 0.16% and 0.49%, corresponding to maximum paleotemperatures of up to ~80 °C. Interestingly, the results cluster at different ranges when grouped according to basin locality. First, VR values for samples from the western part (samples VR1–VR11; Table DR7 [see footnote 1]) vary between 0.22% and 0.32%, corresponding to temperatures of up to 60 °C (Burnham and Sweeney, 1989). No significant differences in maximum paleotemperature were observed between the lowermost Paleocene and the youngest Miocene samples. Estimated burial temperatures of up to 60 °C for sedimentary units as old as early Paleocene have rather low values considering the maximum overburden of 4–5 km, equivalent to the full preserved stratigraphic thickness of the Oligocene to Miocene units younger than the sampled interval. On the other hand, in the eastern part of the Medina Basin, younger units corresponding to the upper members of the Carbonera Formation (C6–C3 members; samples VR12–VR21, Table DR7 [see footnote 1]) yield VR values ranging between 0.35% and 0.45%, corresponding to temperatures of up to 95 °C. The results suggest that strata from the eastern part of the Medina Basin were subjected to higher burial paleotemperatures, not only compared to their lateral equivalents but also in comparison to older units to the west, suggesting nonuniform burial across the basin.

Considering the maximum overburden, the estimated maximum paleotemperatures suggest a mean paleogeothermal gradient of only ~7–9 °C/km for the western area (maximum paleotemperature = ~60 °C; full stratigraphic thickness = ~4–5 km; present surface temperature = 25 °C), a much lower value than the present geothermal gradient of ~22 °C/km, obtained from oil wells in the proximal foredeep of the Llanos Basin (e.g., Bachu et al., 1995). As suggested for similar foreland settings, such as the southeastern margin of the Puna Plateau in NW Argentina (e.g., Coutand et al., 2006), two possible scenarios may explain such an extremely low geothermal gradient. Either it could be related to thermal perturbations driven by expulsion of pore fluids during compaction, caused by rapid syntectonic sedimentation (Deming et al., 1990), or the cooling effects of groundwater recharge driven by an adjacent orographic barrier intercepting moisture (e.g., Forster and Smith, 1989). However, the present geothermal gradient of ~22 °C in an analogous foredeep setting of the Llanos Basin (Bachu et al., 1995) rules out both of these scenarios from having significantly affected the maximum paleotemperature.

Conversely, uneven burial between the eastern and western sectors of the basin, as suggested by the VR data, constitutes compelling evidence for earlier incorporation of the western sector of the basin into the fold-and-thrust belt. This earlier deformation prevented the western Medina Basin from undergoing further burial beneath the stratigraphic thickness as observed farther east, where VR values suggest greater burial. Thus, a previously subsiding area in the western Medina Basin, where the stratigraphic thickness of the C8–C6 members reaches a maximum, became an area of limited accommodation space through structural incorporation into the eastern Andean fold-and-thrust belt.

DISCUSSION AND CONCLUSIONS

Late Eocene-Oligocene History of the Eastern Flank of the Eastern Cordillera

Our data set provides new insights into different evolutionary stages of a foreland fold-and-thrust belt, the compartmentalization of the foreland, and the resulting thermal history of the basin. In particular, we furnish new constraints on the propagation of the northern Andes deformation front during the early stages of Cenozoic mountain building in this part of the orogen. A southwesterly sourced lower Oligocene–lower Miocene eastward-thinning syntectonic wedge composed of the C8–C6 members of the Carbonera Formation was deposited in the Medina Basin during an episode of rapid tectonic subsidence starting at ca. 31 Ma. Rapidly eastward-thinning deposits constituting the upper part of this sedimentary wedge change their character in an eastward direction from alluvial to tidal-influenced coastal plain lithofacies. The age at the top of this stratigraphic interval is biostratigraphically constrained at ca. 22 Ma (Ca7-Ca8 palynozones; Figs. 4 and 5). On the other hand, our ZFT data reveal ongoing early Miocene (ca. 18 Ma) exhumation along the northern termination of the Quetame massif, ~30 km to the west of the Medina Basin. ZFT ages determined from different structural levels on the western flank of the Quetame massif and burial estimates from this area based on vitrinite reflectance data suggest that the ca. 18 Ma ZFT ages obtained from the upper part of the Lower Cretaceous Macanal Formation at least slightly postdate the onset of exhumation. Roughly simultaneous exhumation in the Quetame massif and rapid tectonic subsidence recorded in the upper portion of the syntectonic sedimentary wedge of the Medina Basin thus delineate the position of the orogenic front along the fault system separating the two areas (i.e., the Lengupá-Tesalia fault system) since at least the early Miocene. Furthermore, the apparent disparity between the onset of rapid subsidence at ca. 31 Ma in the Medina

Basin and the younger initiation of exhumation during the early Miocene in the Quetame massif can be explained by the following scenarios: (1) tectonic loads located west of the Quetame massif triggered the stage of rapid subsidence between ca. 31 Ma and the initial exhumation of the Quetame massif shortly before 18 Ma; or (2) the tectonic loads that caused such a rapid subsidence were located in the area of the present-day Quetame massif, and, hence, a significant lag time of as much as 13 m.y. occurred between the emplacement of the thrust loads at ca. 31 Ma and the onset of significant exhumation of the Quetame massif.

Although geodynamic modeling must be conducted to better define the location of the tectonic loads, regional structural and stratigraphic considerations permit us to hypothesize about the most favorable among the two scenarios. Along the axial Eastern Cordillera, an incomplete Cenozoic sedimentary record (see Fig. 2) and incomplete palynological sampling prevent a well-constrained westward extrapolation of sediment accommodation patterns. West of the Medina basin, the easternmost locality where the Paleogene record has been described is in the Usme syncline, south of the High Plain of Bogotá (Fig. 1). There, the Usme Formation consists of 300 m of deltaic deposits (Hoorn et al., 1987) unconformably underlying upper Miocene strata. The available palynological data (Hoorn et al., 1987) reveal that the uppermost 200 m of the Usme Formation correspond to the biozone T-08 (early Oligocene, ca. 34 Ma to 31 Ma). In the composite stratigraphic section of the Medina Basin, the coeval interval in the C8 member of the Carbonera Formation is only ~70 m thick and corresponds to the uppermost part of the Eocene–early Oligocene interval, which registers limited tectonic subsidence (see Table DR6 [see footnote 1]; Fig. 5). These results document faster sediment accumulation and subsidence in the axial part of the Eastern Cordillera compared to the eastern foothills, and they support a scenario of tectonic loading west of the axial part of the Eastern Cordillera prior to 31 Ma. The continuance of this pattern throughout the Oligocene cannot be evaluated due to the incomplete record. However, between the High Plain of Bogotá and the Servitá-Lengupá-Tesalia faults, the structural configuration of the Eastern Cordillera does not involve major faults that could have caused significant tectonic loading (Mora et al., 2006; see also Fig. 1). Thus, we favor the second scenario, in which tectonic loading at ca. 31 Ma was generated by slip along the basement-bounding faults of the Quetame massif, which then caused proximal foredeep deposition in the Medina Basin. In this context, the absence of observable direct indicators of deformation (i.e., growth strata or unconformities) in the forelimbs and backlimbs of the Farallones anticline (Fig. 3) could be explained by poor seismic imaging in the steeply dipping, overturned western limb of the Nazareth syncline and/or subsequent erosion resulting from protracted exhumation and uplift along this structure.

However, despite the absence of such direct indicators, a combination of observed changes in sedimentary facies, thickness, and subsidence patterns in the basin, and the localization of areas with contemporaneous ongoing exhumation enable us to identify the Lengupá-Servitá faults as the most likely locus of the orogenic front since the early Oligocene. Furthermore, the structural configuration of the Lengupá fault and our paleocurrent data from the syntectonic wedge help to place more detailed constraints on the proposed location of the tectonic loads that triggered the earlier phase of subsidence at ca. 31 Ma. The structural cross section across the northern part of the Guavio anticline (Figs. 3B and 8) reveals that the overturned western margin of the basin corresponds to the forelimb of a fault-propagation anticline associated with the northern termination of the Lengupá fault. However, south of the Gazaunta River, deformation along this thrust sheet has been accommodated by faulting (Fig. 3A). This configuration documents a deformation gradient. Nucleation of this fault system appears to have started first in the south, where the fault has attained maximum structural relief. There, pre-Devonian basement rocks have been thrust over upper Cenozoic strata. In contrast, farther north, this fault system only causes folding, and the fault has not yet cut the surface. As illustrated in Figure 8, we suggest that rapid subsidence and increased accommodation in the western part of the basin at ca. 31 Ma would have resulted from loading in the hanging wall of the Servitá-Lengupá thrust sheet to the southwest of the basin. This is further supported by paleocurrent data from the C7–C6 members of the Carbonera Formation, which indicate that the main source for these sediments was located to the southwest of the basin. Subsequent deformation within this thrust sheet propagated northward via fault-propagation folding, which incorporated the western part of the sedimentary wedge into the thrust belt (Fig. 8). The propagation of the structure is also supported by the northward plunge of the Quetame massif. As a result of these processes, the change from subsidence and burial to folding prevented further thermal maturation of organic matter, as revealed by VR data from the C8 member of the Carbonera Formation and younger units in the western Medina Basin. In this context, a difference of ~13 m.y. between the onset of rapid subsidence and the older exhumation ages may result from a combination of (1) an incomplete thermochronologic database, preventing precise identification of the onset of exhumation (thus only representing a minimum age for this process), and (2) a potential temporal lag between thrust loading and exhumation, reflecting the period between the onset of range uplift and significant removal of overburden. More detailed thermochronological investigations in the future might resolve this issue.

Migration of the Foreland Basin System

Our plots of Cenozoic sediment accumulation and tectonic subsidence display a similar three-stage pattern in the southern Middle Magdalena Valley and Medina Basins, resulting from two episodes of rapid subsidence separated by an interval of slower subsidence (Figs. 6A and 6B). In other foreland basins, such three-stage sigmoidal patterns have been explained by vertical superposition of foreland basin depozones resulting from redistribution of thrust loads and progradation of the orogenic wedge (DeCelles and Currie, 1996; Horton et al., 2001). In such a scenario, a cratonward migration of the orogenic wedge results in the superposition of the foredeep, forebulge, and back-bulge depozones. Alternatively, orogenward retreat of the foreland system may lead to vertical stacking of distal (i.e., back-bulge and forebulge) over proximal foreland basin depozones (i.e., foredeep and wedge-top). This latter scenario may result from internal thickening of the orogenic wedge via out-of-sequence reactivation of thrusts in the hinterland (e.g., DeCelles and Giles, 1996), underplating (e.g., Sinclair et al., 1991), or from a decrease in the wavelength of the flexural profile of the basin. Such a decrease can be related to episodic deformation associated with alternating episodes of thrust loading following tectonic quiescence, erosional unloading (Flemings and Jordan, 1990; Burbank, 1992; Catuneanu et al., 1998), or lateral variations in the rigidity of the flexed plate (Waschbusch and Royden, 1992).

Concerning the late Paleocene episode of rapid subsidence during deposition of the Los Cuervos Formation in the Medina Basin, accumulation in a back-bulge depozone can be ruled out in light of the regional distribution of foreland basin deposits. In particular, late Paleocene back-bulge deposition in the Medina Basin would imply that a forebulge would have been located to the west of the basin. However, Paleogene subsidence patterns in the southern Middle Magdalena Valley to the west of the basin do not indicate limited accommodation, such as would be expected in a forebulge depozone. Instead, late Paleocene rapid subsidence in the southern

Middle Magdalena Valley Basin (Fig. 6B) and a thick upper Paleocene sedimentary section in the axial Eastern Cordillera (Cacho Bogotá and Lower and Upper Socha Formations; Fig. 2) result from foredeep deposition related to tectonic loading in the Central Cordillera (Gómez et al., 2003, 2005). We therefore suggest that the rapid accumulation recorded by the Los Cuervos deposits in the Medina Basin reflects deposition in the eastern reaches of this foredeep depozone. However, as noted by Sarmiento-Rojas (2001), a minor contribution of remaining thermal subsidence from a Mesozoic rifting event may account for part of the observed rapid tectonic subsidence in the basin. As pointed out by Gómez et al. (2005), eastward onlapping of the late Paleocene Barco and Los Cuervos Formations onto the Cenozoic and Mesozoic substratum of the Llanos Basin suggests an increase in the wavelength of the foreland basin (i.e., basin widening; see Figs. 2 and 9C) that may correlate with a diminished load exerted by the Central Cordillera. The adjustment of the flexural profile of the basin to such episodes of erosional unloading is characterized by an increase in subsidence in the distal foreland basin system (i.e., in the forebulge) that correlates with diminished subsidence or flexural uplift in the foredeep (e.g., Burbank, 1992; Catuneanu et al., 1997, 1998). Although limited, data from the northern part of the Middle Magdalena Valley Basin (Pardo-Trujillo et al., 2003) suggest a decrease in sediment accumulation rates toward the top of the upper Paleocene units. This may represent a reduction in subsidence within a proximal foredeep coeval with the increase in subsidence rates that allowed the accumulation and eastward onlapping of the Barco and Los Cuervos Formations over more distal foredeep areas pre-

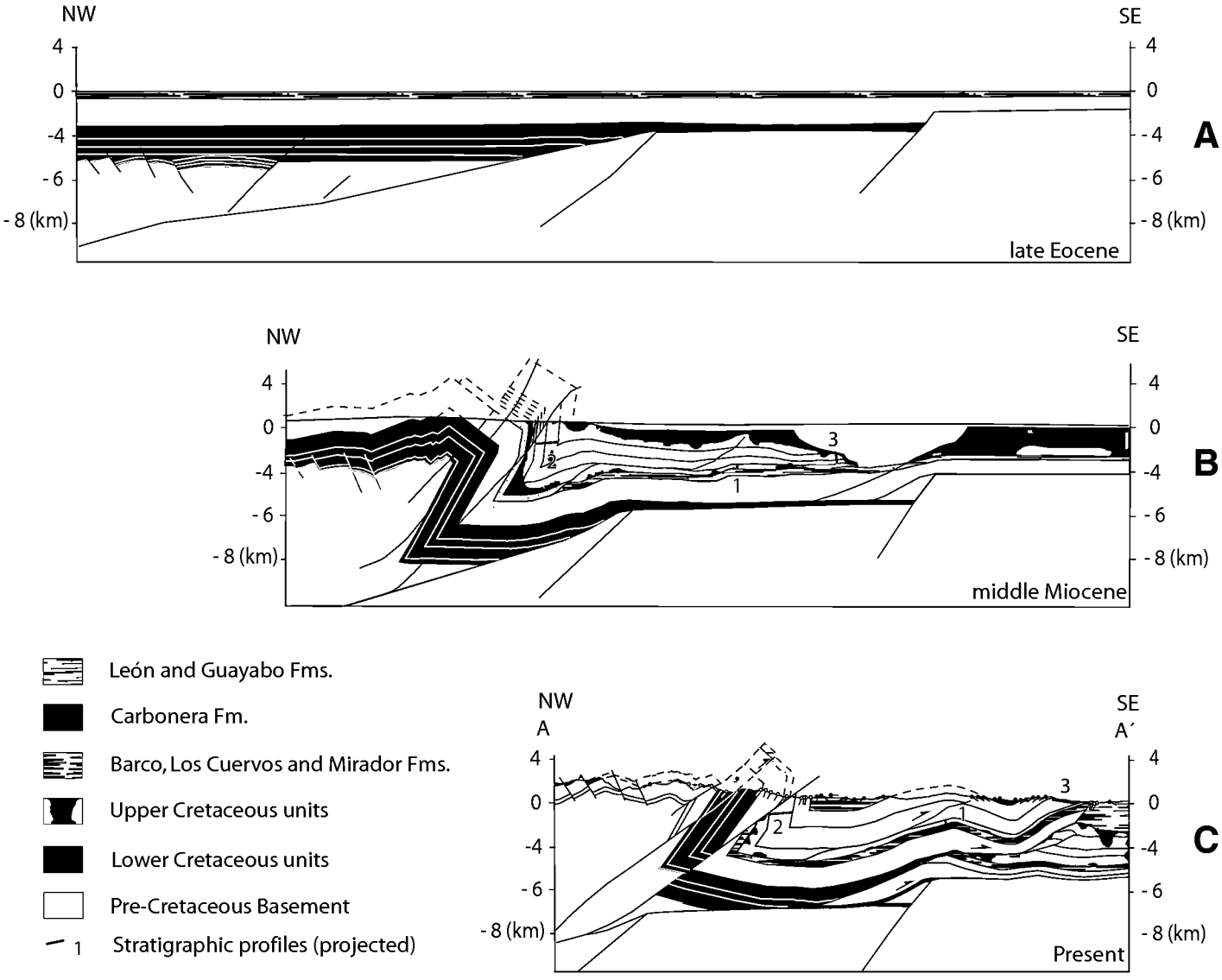

Figure 8. Retrodeformed cross section across the Medina Basin during (A) late Eocene, (B) early Miocene, and (C) present time, respectively (location of cross section in Fig. 2). Projected locations of stratigraphic sections and samples for vitrinite reflectance and zircon fission-track analysis are indicated for each time slice. Thrust-induced exhumation along of the Quetame massif during early Miocene incorporated the western part of the syntectonic clastic wedge of the Medina Basin into the fold-and-thrust belt. This resulted in the interruption of the thermal maturation of strata rich in organic matter in the western Medina Basin.

viously subjected to erosion in the Llanos Basin (Gómez et al., 2005) (Fig. 9).

We interpreted the intermediate stage of reduced accumulation in the Medina Basin during the Eocene–early Oligocene (ca. 56–31 Ma) using a regional comparison of accommodation patterns across the foreland basin system. This stage of moderate subsidence rates in the Medina Basin was coeval with late Paleocene to middle Eocene unconformity development in the Middle Magdalena Valley Basin (Restrepo-Pace et al., 2004; Gómez et al., 2005). In the southern part of the southern Middle Magdalena Valley Basin, such an episode is represented by the flat segment in the subsidence curve (Fig. 6B). Subsequent uplift in the western part of the Eastern Cordillera documented by AFT modeling and middle Eocene–Oligocene growth strata in the southern part of the basin also overlaps in time with the episode of limited accommodation recorded by the Eocene–lower Oligocene deposits of the Medina Basin. We suggest that such limited accommodation, subsequent to a late Paleocene episode of rapid subsidence, which we interpret to have occurred in a foredeep depozone, is compatible with a distal foredeep setting. In this context, we invoke a reduction in tectonic subsidence, which reveals an episode of basin narrowing and westward retreat of the foreland basin system (Fig. 9D). Moreover, in the east, the development of an unconformity with an eastward-increasing chronostratigraphic gap beneath the middle Eocene Mirador Formation (Jaramillo et al., 2008) suggests the existence of a forebulge in the Llanos Basin at that time. Following the late Paleocene episode of faster subsidence in the course of erosional unloading, limited Eocene accumulation in the eastern foothills can be interpreted as a flexural response of the basin to a renewed episode of thrust loading. This may have resulted from the eastward migration of the Central Cordillera thrust front as well as the onset of thrusting along the western flanks of the Eastern Cordillera (Fig. 9D). Interestingly, available palynological data from the northern Magdalena Valley Basin (Pardo-Trujillo et al., 2003) show a coeval, yet opposite pattern of increased sediment accommodation between the Paleocene and Eocene, which is in line with asymmetric subsidence as a response to renewed thrust loading and basin narrowing. This long-lasting (ca. 25 m.y.) episode of slower subsidence and narrowing of the Medina Basin may also suggest protracted stationary foredeep and forebulge depozones. Such stagnation of the foreland system may have been the consequence of tectonic loading acting over a less rigid part of the foreland lithosphere (e.g., Waschbusch and Royden, 1992). In this case, the weakened lithosphere could correspond to a prestrained

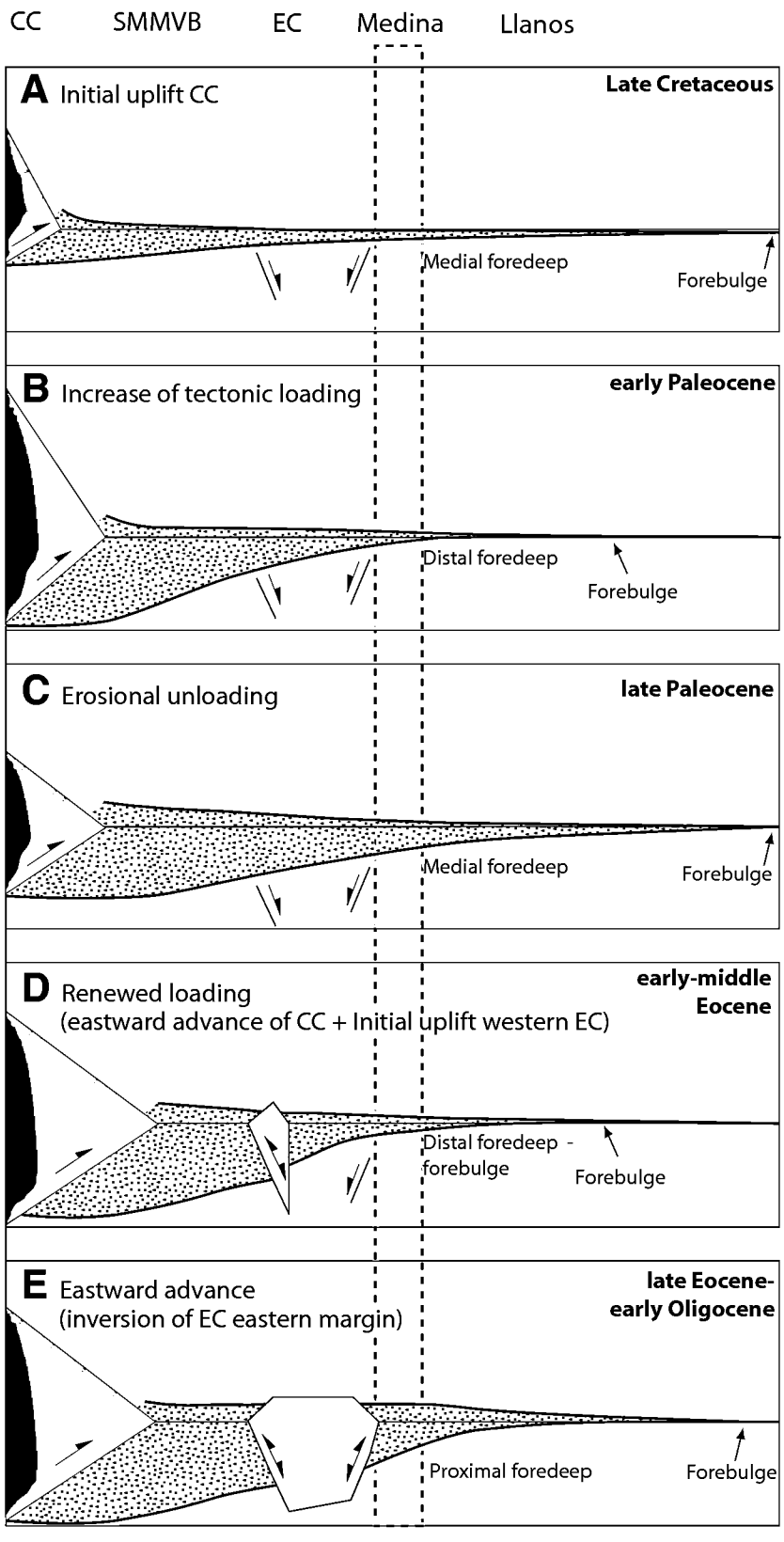

Figure 9. Cartoon illustrating the Maastrichtian–early Oligocene evolution of the foreland basin system in response to uplift of the Central (CC) and Eastern (EC) Cordilleras of the Colombian Andes. SMMVB—southern Middle Magdalena Valley Basin. See text for discussion.

area affected by Mesozoic rifting, which now delimits the extent of the Eastern Cordillera (Fabre, 1983; Sarmiento-Rojas et al., 2006). However, a comprehensive regional documentation of Cenozoic exhumation patterns and geodynamical modeling are required to further test the validity of these hypotheses.

Finally, the second stage of rapid subsidence in the Medina Basin, starting in the early Oligocene, documents proximal foredeep deposition due to loading through initial inversion of the Servitá fault (Figs. 8 and 9E). This episode thus reveals a stage of basinward migration of the foreland basin system that involved the reactivation of inherited Cretaceous extensional faults. Moreover, this early initiation of thrusting along the Servitá-Lengupá fault in the early Oligocene documents protracted deformation located along this reactivated fault. This is in line with active thrust-induced exhumation throughout the Miocene, suggested by the ZFT data, and rapid exhumation during the last ~3 m.y., as indicated by apatite fission-track data in the Quetame massif (Mora et al., 2008a). Our data thus provide compelling evidence for the fundamental role exerted by inherited basement anisotropies in accommodating contractional deformation during Cenozoic orogenesis in the northern Andes. The Eastern Cordillera of the Colombian Andes hence constitutes a natural testing ground for numerical models predicting the locus of active deformation in an orogen as determined to a great extent by weak zones in the crust that accommodate shortening. However, as predicted by Allmendinger et al. (1983), more straightforward time-space patterns of deformation associated with an orogenic wedge may develop in those areas where the role of such anisotropies is reduced or where pre-existing basin fills provide a much more homogeneous material to develop new detachment systems that promote systematic lateral orogenic growth.

In summary, our new data from the Medina Basin provide evidence for the initial stages of mountain building and foreland basin development along the eastern margin of the Eastern Cordillera of the Colombian Andes. Our model of foreland basin development provides a consistent hypothesis for a variety of observations, including the spatiotemporal patterns of subsidence, sediment dispersal in the basin, and exhumation patterns in the hinterland. Our multidisciplinary study has identified the early Eocene to early Miocene locus of deformation and flexural loading in the Eastern Cordillera of the central Colombia Andes, and it correlates the response of the foreland basin to the tectonic activity of individual thrust sheets. Our data support previous hypotheses suggesting episodic deformation in this environment as the principal mechanism controlling foreland dynamics up to late Paleocene time. Likewise, we suggest that this mechanism was gradually replaced by a combination of renewed loading in the Central Cordillera and eastward migration of the deformation front to the western foothills of the Eastern Cordillera during Eocene–early Oligocene time. Finally, ~31 m.y. ago, the orogenic front would have shifted eastward, and deformation would have been accommodated along an inherited Mesozoic extensional structure. The behavior of the foreland basin of the Colombian Andes thus resembles other foreland regions of the Andean orogen (Mon and Salfity, 1995; Hilley et al., 2005; Carrera et al., 2006; Hain and Strecker, 2008), where predicted patterns of gradual, foreland-directed migration of deformation are modified by the effects of loading of inherited crustal weak zones, the activation of which generates a much more complex pattern of thrust-belt evolution.

ACKNOWLEDGMENTS

This research was supported by grants and scholarships from the German Academic Exchange Service (scholarships A/02/11325 and A/01/12054 to M. Parra and A. Mora, respectively), Deutsche Forschungsgemeinschaft (DFG; Str 373/19-1 to M. Strecker), funds from the DFG-Leibniz Center for Earth Surface and Climate Studies at Potsdam University, and the Universidad Nacional de Colombia (Beca de Honor to M. Parra). We also thank the Instituto Colombiano del Petróleo and the Smithsonian Tropical Research Institute for financial support. Seismic profiles were kindly provided by the ANH (Agencia Nacional de Hidrocarburos) of Colombia. We thank B. Horton, G. Bayona, and C. Uba for discussions that helped improve the paper. We also greatly appreciate discussions with A. Kammer and E. López on the Cenozoic stratigraphy of the area. N. Cardozo generously provided us with his program OSXBackstrip for one-dimensional backstripping. A. Gómez kindly identified fossils. G. Veloza and R. López are thanked for their assistance in the field. We are grateful for thorough reviews by D. Barbeau, M. Giovanni, and E. Gómez, and helpful suggestions by Associate Editor J. Schmitt.

REFERENCES CITED

Allen, P.A., and Allen, J.R., 2005, Basin Analysis: Principles and Applications: Oxford, Blackwell Science, 549 p.

Allmendinger, R.W., Ramos, V.A., Jordan, T.E., Palma, M., and Isacks, B.L., 1983, Paleogeography and Andean structural geometry, northwest Argentina: Tectonics, v. 2, no. 1, p. 1–16, doi: 10.1029/TC002i001p00001.

Angevine, C.L., Heller, P.L., and Paola, C., 1993, Quantitative Sedimentary Basin Modelling, American Association of Petroleum Geologists Course Note Series 32, 132 p.

Bachu, S., Ramon, J.C., Villegas, M.E., and Underschultz, J.R., 1995, Geothermal regime and thermal history of the Llanos Basin, Colombia: The American Association of Petroleum Geologists Bulletin, v. 79, no. 1, p. 116–129.

Barker, C.E., and Pawlewicz, M.J., 1993, An empirical determination of the minimum number of measurements needed to estimate the mean random vitrinite reflectance of disseminated organic matter: Organic Geochemistry, v. 20, no. 6, p. 643–651, doi: 10.1016/0146-6380(93)90050-L.

Bayona, G., Reyes-Harker, A., Jaramillo, C.A., Rueda, M., Aristizabal, J., Cortés, M., and Gamba, N., 2006, Distinguishing tectonic versus eustatic surfaces in the Llanos Basin of Colombia, and implications for stratigraphic correlations, *in* Asociación Colombiana de Geólogos y Geofísicos del Petróleo ed., Extended Abstracts, IX Simposio Bolivariano de Exploración Petrolera en las Cuencas Subandinas: Cartagena de Indias, Colombia, 13 p.

Beaumont, C., 1981, Foreland basins: Geophysical Journal of the Royal Astronomical Society, v. 65, p. 291–329.

Bernet, M., and Garver, J.I., 2005, Fission-track analysis of detrital zircon: Reviews in Mineralogy and Geochemistry, v. 58, p. 205–238, doi: 10.2138/rmg.2005.58.8.

Burbank, D.W., 1992, Causes of recent Himalayan uplift deduced from depositional patterns in the Ganges basin: Nature, v. 357, p. 680–682, doi: 10.1038/357680a0.

Burnham, A.K., and Sweeney, J.J., 1989, A chemical kinetic model of vitrinite maturation and reflectance: Geochimica et Cosmochimica Acta, v. 53, no. 10, p. 2649–2657, doi: 10.1016/0016-7037(89)90136-1.

Campbell, C.J., and Bürgl, H., 1965, Section through the Eastern Cordillera of Colombia, South America: Geological Society of America Bulletin, v. 76, no. 5, p. 567–590, doi: 10.1130/0016-7606(1965)76[567:STTECO]2.0.CO;2.

Carrera, N., Muñoz, J.A., Sàbat, F., Mon, R., and Roca, E., 2006, The role of inversion tectonics in the structure of the Cordillera Oriental (NW Argentinean Andes): Journal of Structural Geology, v. 28, no. 11, p. 1921–1932, doi: 10.1016/j.jsg.2006.07.006.

Catuneanu, O., Beaumont, C., and Waschbusch, P., 1997, Interplay of static loads and subduction dynamics in foreland basins: Reciprocal stratigraphies and the "missing" peripheral bulge: Geology, v. 25, no. 12, p. 1087–1090, doi: 10.1130/0091-7613(1997)025<1087:IOSLAS>2.3.CO;2.

Catuneanu, O., Hancox, P.J., and Rubidge, B.S., 1998, Reciprocal flexural behaviour and contrasting stratigraphies: A new basin development model for the Karoo retroarc foreland system, South Africa: Basin Research, v. 10, no. 4, p. 417–439, doi: 10.1046/j.1365-2117.1998.00078.x.

Cazier, E.C., Cooper, M.A., Eaton, S.G., and Pulham, A.J., 1997, Basin development and tectonic history of the Llanos Basin, Eastern Cordillera, and Middle Magdalena Valley, Colombia: The American Association of Petroleum Geologists Bulletin, v. 81, no. 8, p. 1332–1338.

Coleman, J.M., Roberts, H.H., and Stone, G.W., 1998, Mississippi River delta: An overview: Journal of Coastal Research, v. 14, no. 3, p. 698–716.

Colletta, B., Hebrard, F., Letouzey, J., Werner, P., and Rudkiweicz, J.L., 1990, Tectonic style and crustal structure of the Eastern Cordillera, Colombia, from a balanced cross section, *in* Letouzey, J., ed., Petroleum and Tectonics in Mobile Belts: Paris, Editions Technip, p. 81–100.

Cooper, M. A., Addison, F. T., Álvarez, R., Coral, M., Graham, R. H., Hayward, S. H., Martínez, J., Naar, J., Peñas, R., Pulham, A. J., and Taborda, A., 1995, Basin development and tectonic history of the Llanos Basin, Eastern Cordillera, and Middle Magdalena Valley, Colombia: American Association of Petroleum Geologists Bulletin, v. 79, no. 10, p. 1421-1443.

Corredor, F., 2003, Eastward extent of the late Eocene–early Oligocene onset of deformation across the northern Andes: Constraints from the northern portion of the Eastern Cordillera fold belt, Colombia: Journal of South American Earth Sciences, v. 16, no. 6, p. 445–457, doi: 10.1016/j.jsames.2003.06.002.

Coutand, I., Cobbold, P. R., De Urreiztieta, M., Gautier, P., Chauvin, A., Gapais, D., Rossello, E. A., and López-Gamundi, O., 2001, Style and history of Andean deformation, Puna Plateau, northwestern Argentina: Tectonics, v. 20, no. 2, p. 210–234, doi: 10.1029/2000TC900031.

Coutand, I., Carrapa, B., Deeken, A., Schmitt, A.K., Sobel, E.R., and Strecker, M.R., 2006, Propagation of orographic barriers along an active range front: Insights from sandstone petrography and detrital apatite fission-

track thermochronology in the intramontane Angastaco Basin, NW Argentina: Basin Research, v. 18, no. 1, p. 1–26, doi: 10.1111/j.1365-2117.2006.00283.x.

Damanti, J.F., 1993, Geomorphic and structural controls on facies patterns and sediment composition in a modern foreland basin, *in* Marzo, M., and Puigdefábregas, C., eds., Alluvial Sedimentation: International Association of Sedimentologists Special Publication 17, p. 221–233.

Dávila, F.M., and Astini, R.A., 2003, Early middle Miocene broken foreland development in the southern Central Andes: Evidence for extension prior to regional shortening: Basin Research, v. 15, no. 3, p. 379–396, doi: 10.1046/j.1365-2117.2003.00206.x.

DeCelles, P.G., 2004, Late Jurassic to Eocene evolution of the Cordilleran thrust belt and foreland basin system, western U.S.: American Journal of Science, v. 304, no. 2, p. 105–168, doi: 10.2475/ajs.304.2.105.

DeCelles, P.G., and Currie, B.S., 1996, Long-term sediment accumulation in the middle Jurassic–early Eocene Cordilleran retroarc foreland-basin system: Geology, v. 24, no. 7, p. 591–594, doi: 10.1130/0091-7613(1996)024<0591:LTSAIT>2.3.CO;2.

DeCelles, P.G., and Giles, K.A., 1996, Foreland basin systems: Basin Research, v. 8, no. 2, p. 105–123, doi: 10.1046/j.1365-2117.1996.01491.x.

DeCelles, P.G., Langford, R.P., and Schwartz, R.K., 1983, Two new methods of paleocurrent determination from trough cross-stratification: Journal of Sedimentary Petrology, v. 53, no. 2, p. 629–642.

DeCelles, P.G., Gehrels, G.E., Quade, J., Ojha, T.P., Kapp, P.A., and Upreti, B.N., 1998, Neogene foreland basin deposits, erosional unroofing, and the kinematic history of the Himalayan fold-thrust belt, western Nepal: Geological Society of America Bulletin, v. 110, no. 1, p. 2–21, doi: 10.1130/0016-7606(1998)110<0002:NFBDEU>2.3.CO;2.

Deming, D., Nunn, J.A., and Evans, D.G., 1990, Thermal effects of compaction-driven groundwater flow from overthrust belts: Journal of Geophysical Research, v. 95, no. B5, p. 6669–6683, doi: 10.1029/JB095iB05p06669.

Dengo, C.A., and Covey, M.C., 1993, Structure of the Eastern Cordillera of Colombia: Implications for trap styles and regional tectonics: American Association of Petroleum Geologists Bulletin, v. 77, no. 8, p. 1315–1337.

Duque-Caro, H., 1990, The Choco block in the northwestern corner of South America: Structural, tectonostratigraphic and paleogeographic implications: Journal of South American Earth Sciences, v. 3, p. 71–84, doi: 10.1016/0895-9811(90)90019-W.

Echavarria, L., Hernández, R., Allmendinger, R., and Reynolds, J., 2003, Subandean thrust and fold belt of northwestern Argentina: Geometry and timing of the Andean evolution: The American Association of Petroleum Geologists Bulletin, v. 87, no. 6, p. 965–985.

Einsele, G., 2000, Sedimentary Basins: Evolution, Facies and Sedimentary Budget: Heidelberg, Springer Verlag, 781 p.

Fabre, A., 1983, La subsidencia de la Cuenca del Cocuy (Cordillera Oriental de Colombia) durante el Cretáceo y el Terciario Inferior. Primera parte: Estudio cuantitativo de la subsidencia: Geología Norandina, v. 8, p. 22–27.

Flemings, P.B., and Jordan, T.E., 1989, A synthetic stratigraphic model of foreland basin development: Journal of Geophysical Research, v. 94, no. B4, p. 3851–3866, doi: 10.1029/JB094iB04p03851.

Flemings, P.B., and Jordan, T.E., 1990, Stratigraphic modeling of foreland basins: Interpreting thrust deformation and lithosphere rheology: Geology, v. 18, p. 430–434, doi: 10.1130/0091-7613(1990)018<0430:SMOFBI>2.3.CO;2.

Forster, C., and Smith, L., 1989, The influence of groundwater flow on thermal regimes in mountainous terrain: A model study: Journal of Geophysical Research, v. 94, no. B7, p. 9439–9451, doi: 10.1029/JB094iB07p09439.

Galbraith, R.F., 1981, On statistical models for fission-tracks counts: Mathematical Geology, v. 13, no. 6, p. 471–478, doi: 10.1007/BF01034498.

Germeraad, J.H., Hopping, C.A., and Muller, J., 1968, Palynology of Tertiary sediments from tropical areas: Review of Palaeobotany and Palynology, v. 6, p. 189–198, doi: 10.1016/0034-6667(68)90051-1.

Gómez, E., Jordan, T.E., Allmendinger, R.W., Hegarty, K., Kelley, S., and Heizler, M., 2003, Controls on architecture of the Late Cretaceous to Cenozoic southern Middle Magdalena Valley Basin, Colombia: Geological Society of America Bulletin, v. 115, no. 2, p. 131–147, doi: 10.1130/0016-7606(2003)115<0131:COAOTL>2.0.CO;2.

Gómez, E., Jordan, T.E., Allmendinger, R.W., and Cardozo, N., 2005, Development of the Colombian foreland-basin system as a consequence of diachronous exhumation of the northern Andes: Geological Society of America Bulletin, v. 117, no. 9–10, p. 1272–1292, doi: 10.1130/B25456.1.

Gradstein, F.M., Ogg, J.G., Smith, A.G., Bleeker, W., and Lourens, L.J., 2004, A new geologic time scale, with special reference to Precambrian and Neogene: Episodes, v. 27, no. 2, p. 83–100.

Green, P.F., 1981, A new look at statistics in fission-track dating: Nuclear Tracks, v. 5, p. 77–86, doi: 10.1016/0191-278X(81)90029-9.

Green, P.F., Duddy, I.R., Gleadow, A.J.W., Tingate, P.R., and Laslett, G.M., 1986, Thermal annealing of fission tracks in apatite: 1. A qualitative description: Chemical Geology, v. 59, no. 4, p. 237–253, doi: 10.1016/0009-2541(86)90048-3.

Guidish, T.M., Kendall, C.G.S.C., Lerche, I., Toth, D.J., and Yarzab, R.F., 1985, Basin evaluation using burial history calculations: An overview: American Association of Petroleum Geologists Bulletin, v. 69, no. 1, p. 92–105.

Hain, M.P., and Strecker, M.R., 2008, The control of Cretaceous extension and pre-existing basement structures upon position and style of Andean shortening—A case study from the Valle de Lerma, Salta, NW Argentina, *in* Asociación Geológica Argentina ed., XVII Congreso Geológico Argentino: San Salvador de Jujuy, Argentina (in press).

Haq, B.U., Hardenbol, J., and Vail, P.R., 1987, Chronology of fluctuating sea levels since the Triassic: Science, v. 235, no. 4793, p. 1156–1167, doi: 10.1126/science.235.4793.1156.

Helmens, K.F., and Van der Hammen, T., 1994, The Pliocene-Quaternary of the high plain of Bogotá: A history of tectonic uplift, basin development and climatic change: Quaternary International, v. 21, p. 41–61, doi: 10.1016/1040-6182(94)90020-5.

Hilley, G. E., Strecker, M. R., and Ramos, V. A., 2004, Growth and erosion of fold-and-thrust belts with an application to the Aconcagua fold-and-thrust belt, Argentina: Journal of Geophysical Research B: Solid Earth, v. 109, B01410, doi:10.1029/2002JB002282.

Hoorn, C., Kaandorp, M.C.N., and Roele, J., 1987, Tertiary sediments of the Usme Valley, Colombia: A palynological and stratigraphical approach: Hugo de Vries Laboratory, University of Amsterdam, Amsterdam, 31 p.

Horton, B.K., 1999, Erosional control on the geometry and kinematics of thrust belt development in the central Andes: Tectonics, v. 18, no. 6, p. 1292–1304, doi: 10.1029/1999TC900051.

Horton, B.K., 2005, Revised deformation history of the central Andes: Inferences from Cenozoic foredeep and intermontane basins of the Eastern Cordillera, Bolivia: Tectonics, v. 24, no. 3, TC3011, doi: 10.1029/2003TC001619.

Horton, B.K., Hampton, B.A., and Waanders, G.L., 2001, Paleogene synorogenic sedimentation in the Altiplano plateau and implications for initial mountain building in the Central Andes: Geological Society of America Bulletin, v. 113, no. 11, p. 1387–1400, doi: 10.1130/0016-7606(2001)113<1387:PSSITA>2.0.CO;2.

Huntington, K.W., Ehlers, T.A., Hodges, K.V., and Whipp, D.M., 2007, Topography, exhumation pathway, age uncertainties, and the interpretation of thermochronometer data: Tectonics, v. 26, p. TC4012, doi: 10.1029/2007TC002108.

Jaramillo, C., and Dilcher, D.L., 2000, Microfloral diversity patterns of the late Paleocene–Eocene interval in Colombia, northern South America: Geology, v. 28, no. 9, p. 815–818, doi: 10.1130/0091-7613(2000)28<815:MDPOTL>2.0.CO;2.

Jaramillo, C., and Dilcher, D.L., 2001, Middle Paleogene palynology of Central Colombia, South America: A study of pollen and spores from tropical latitudes: Palaeontographica B, v. 258, p. 87–213.

Jaramillo, C., and Rueda, M., 2004, Impact of biostratigraphy in oil exploration, *in* Asociación Colombiana de Geólogos y Geofísicos del Petróleo ed., Abstracts, III Covencion Técnica Asociación Colombiana de Geólogos y Geofísicos del Petróleo: Bogotá, 6 p.

Jaramillo, C., Muñoz, F., Cogollo, M., and Parra, F., 2005, Quantitative biostratigraphy for the Paleocene of the Llanos foothills, Colombia: Improving palynological resolution for oil exploration, *in* Powell, A.J., and Riding, J., eds., Recent Developments in Applied Biostratigraphy: Micropalaeontological Society Special Publication TMS001, p. 145–159.

Jaramillo, C., Rueda, M., and Mora, G., 2006, Cenozoic plant diversity in the Neotropics: Science, v. 311, p. 1893–1896, doi: 10.1126/science.1121380.

Jaramillo, C., Pardo-Trujullo, A., Rueda, M., Harrington, G., Bayona, G., Torres, V., and Mora, G., 2007, Palynology of the Upper Paleocene Cerrejon Formation, northern Colombia: Palynology, v. 31, p. 153–189, doi: 10.2113/gspalynol.31.1.153.

Jaramillo, C., Rueda, M., Bayona, G., Santos, C., Florez, P., and Parra, F., 2008, Biostratigraphy breaking paradigms: dating the Mirador Formation in the Llanos Basin of Columbia, *in* Demchuk, T., and Waszczak, R., eds., Geologic Problem Solving with Microfossils, Society for Sedimentary Geology Special Publication (in press).

Jordan, T.E., 1981, Thrust loads and foreland basin evolution, Cretaceous, western United States: American Association of Petroleum Geologists Bulletin, v. 65, p. 2506–2520.

Jordan, T.E., 1995, Retroarc foreland and related basins, *in* Busby, C.J., and Ingersoll, R.V., eds., Tectonic of Sedimentary Basins: Cambridge, Massachusetts, Blackwell Science, p. 331–362.

Jordan, T.E., Allmendinger, R.W., Damanti, J.F., and Drake, R.E., 1993, Chronology of motion in a complete thrust belt: the Precordillera, 30–31°S, Andes Mountains: The Journal of Geology, v. 101, no. 2, p. 135–156.

Julivert, M., 1963, Los rasgos tectónicos de la región de la Sabana de Bogotá y los mecanismos de la formación de las estructuras: Boletín de Geología, Universidad Industrial de Santander, v. 13–14, p. 5–102.

Kammer, A., 2003, La Formación Tilatá en los alrededores de Chocontá: Marco tectónico y ambientes deposicionales: Análisis Geográficos, v. 26, p. 69–100.

Kammer, A., and Sánchez, J., 2006, Early Jurassic rift structures associated with the Soapaga and Boyacá faults of the Eastern Cordillera, Colombia: Sedimentological inferences and regional implications: Journal of South American Earth Sciences, v. 21, no. 4, p. 412–422, doi: 10.1016/j.jsames.2006.07.006.

Lowe, D.R., 1975, Water escape structures in coarse-grained sediments: Sedimentology, v. 22, p. 157–204, doi: 10.1111/j.1365-3091.1975.tb00290.x.

Martínez, J., 2006, Structural evolution of the Llanos foothills, Eastern Cordillera, Colombia: Journal of South American Earth Sciences, v. 21, no. 4, p. 510–520, doi: 10.1016/j.jsames.2006.07.010.

McCourt, W. J., Aspden, J. A., and Brook, M., 1984, New geological and chronological data from the Colombian Andes: Continental growth by multiple accretion: Journal of the Geological Society of London, v. 141, p. 831–845.

Miall, A.D., 1996, The Geology of Fluvial Deposits: Sedimentary Facies, Basin Analysis, and Petroleum Geology: New York, Springer, 582 p.

Mojica, J., Kammer, A., and Ujueta, G., 1996, El Jurásico del sector noroccidental de Suramérica: Geología Colombiana, v. 21, p. 3–40.

Mon, R., and Salfity, J.A., 1995, Tectonic evolution of the Andes of northern Argentina, *in* Tankard, A.J., Suarez, R., and Welsink, H.J., eds., Petroleum Basins of South America: American Association of Petroleum Geologists Memoir 62, p. 269–283.

Montes, C., Hatcher, R.D., Jr., and Restrepo-Pace, P.A., 2005, Tectonic reconstruction of the northern Andean blocks: Oblique convergence and rotations derived from the kinematics of the Piedras-Girardot area, Colombia: Tectonophysics, v. 399, no. 1–4, p. 221–250, doi: 10.1016/j.tecto.2004.12.024.

Mora, A., Parra, M., Strecker, M.R., Kammer, A., Dimaté, C., and Rodríguez, F., 2006, Cenozoic contractional

reactivation of Mesozoic extensional structures in the Eastern Cordillera of Colombia: Tectonics, v. 25, no. 2, TC2010, doi: 10.1029/2005TC001854.

Mora, A., Parra, M., Strecker, M.R., Sobel, E.R., Hooghiemstra, H., Torres, V., and Vallejo-Jaramillo, J., 2008a, Climatic forcing of asymmetric orogenic evolution in the Eastern Cordillera of Colombia: Geological Society of America Bulletin, v. 120, no. 7–8, p. 930–949, doi: 10.1130/B26186.1.

Mora, A., Gaona, T., Kley, J., Montoya, D., Parra, M., Quiroz, L.I., Reyes, G., and Strecker, M., 2008b, The role of inherited extensional fault segmentation and linkage in contractional orogenesis: A reconstruction of Lower Cretaceous inverted rift basin in the Eastern Cordillera of Colombia: Basin Research (in press).

Mortimer, E., Carrapa, B., Coutand, I., Schoenbohm, L., Sobel, E.R., Gomez, J.S., and Strecker, M.R., 2007, Fragmentation of a foreland basin in response to out-of-sequence basement uplifts and structural reactivation: El Cajon–Campo del Arenal Basin, NW Argentina: Geological Society of America Bulletin, v. 119, no. 5–6, p. 637–653, doi: 10.1130/B25884.1.

Muller, J., Di Giacomo, E., and Van Erve, A., 1987, A palynologic zonation for the Cretaceous, Tertiary and Quaternary of northern South America: American Association of Stratigraphic Palynologist: Contribution Series, v. 19, p. 7–76.

Nuttall, C.P., 1990, A review of the Tertiary non-marine molluscan faunas of the Pebasian and other inland basins of north-western South America: Bulletin of the British Museum (Natural History)–Geology Series, v. 45, no. 2, p. 165–371.

Ojeda, G.Y., Bayona, G., Pinilla, J., Cortés, M., and Gamba, N., 2006, Subsidence and geodynamic analysis of the Llanos Basin: Linking mountain building and basin filling processes, *in* Asociación Colombiana de Geólogos y Geofísicos del Petróleo, ed., Extended Abstracts, IX Simposio Bolivariano de Exploración Petrolera en las Cuencas Subandinas: Cartagena de Indias, Colombia, 12 p.

Owen, G., 1996, Experimental soft-sediment deformation: Structures formed by the liquefaction of unconsolidated sands and some ancient examples: Sedimentology, v. 43, no. 2, p. 279–293, doi: 10.1046/j.1365-3091.1996.d01-5.x.

Pardo-Trujillo, A., Jaramillo, C., and Oboh-Ikuenobe, F.E., 2003, Paleogene palynostratigraphy of the eastern Middle Magdalena Valley, Colombia: Palynology, v. 27, p. 155–178, doi: 10.2113/27.1.155.

Raasveldt, H.C., 1956, Mapa Geológico de la República de Colombia, Plancha L9 (Girardot): Bogotá, Instituto Geológico Nacional, scale 1:200,000.

Ramon, J.C., and Rosero, A., 2006, Multiphase structural evolution of the western margin of the Girardot subbasin, Upper Magdalena Valley, Colombia: Journal of South American Earth Sciences, v. 21, no. 4, p. 493–509, doi: 10.1016/j.jsames.2006.07.012.

Ramos, V.A., Cristallini, E.O., and Pérez, D.J., 2002, The Pampean flat-slab of the Central Andes: Journal of South American Earth Sciences, v. 15, no. 1, p. 59–78, doi: 10.1016/S0895-9811(02)00006-8.

Restrepo-Pace, P.A., Colmenares, F., Higuera, C., and Mayorga, M., 2004, A fold-and-thrust belt along the western flank of the Eastern Cordillera of Colombia. Style, kinematics, and timing constraints derived from seismic data and detailed surface mapping, *in* McClay, K.R., ed., Thrust Tectonics and Hydrocarbon Systems: American Association of Petroleum Geologists Memoir 82, p. 598–613.

Sarmiento-Rojas, L.F., 2001, Mesozoic Rifting and Cenozoic Basin Inversion History of the Eastern Cordillera, Colombian Andes [Ph.D. thesis]: Amsterdam,Vrije University, 295 p.

Sarmiento-Rojas, L.F., Van Wess, J.D., and Cloetingh, S., 2006, Mesozoic transtensional basin history of the Eastern Cordillera, Colombian Andes: Inferences from tectonic models: Journal of South American Earth Sciences, v. 21, no. 4, p. 383–411, doi: 10.1016/j.jsames.2006.07.003.

Sinclair, H.D., 1997, Tectonostratigraphic model for underfilled peripheral foreland basins: An Alpine perspective: Geological Society of America Bulletin, v. 109, no. 3, p. 324–346, doi: 10.1130/0016-7606(1997)109<0324:TMFUPF>2.3.CO;2.

Sinclair, H.D., Coakley, B.J., Allen, P.A., and Watts, A.B., 1991, Simulation of foreland basin stratigraphy using a diffusion model of mountain belt uplift and erosion: An example from the central Alps, Switzerland: Tectonics, v. 10, no. 3, p. 599–620, doi: 10.1029/90TC02507.

Tagami, T., and O'Sullivan, P.B., 2005, Fundamentals of fission-track thermochronology: Reviews in Mineralogy and Geochemistry, v. 58, p. 19–47, doi: 10.2138/rmg.2005.58.2.

Tagami, T., Galbraith, R.F., Yamada, R., and Laslett, G.M., 1998, Revised annealing kinetics of fission tracks in zircon and geological implications, *in* Van den Haute, P., and De Corte, F., eds., Advances in Fission-Track Geochronology: Dordrecht, Kluwer Academic Publishers, p. 99-112.

Tissot, B.P., Pelet, R., and Ungerer, P., 1987, Thermal history of sedimentary basins, maturation indices, and kinetics of oil and gas generations: American Association of Petroleum Geologists Bulletin, v. 71, no. 12, p. 1445–1466.

Toro, J., Roure, F., Bordas-Le Floch, N., Le Cornec-Lance, S., and Sassi, W., 2004, Thermal and kinematic evolution of the Eastern Cordillera fold and thrust belt, Colombia, *in* Swennen, R., Roure, F., and Granath, J.W., eds., Deformation, Fluid Flow, and Reservoir Appraisal in Foreland Fold and Thrust Belts: American Association of Petroleum Geologists Hedberg Series 1, p. 79–115.

Traverse, A., 1988, Paleopalynology: New York, Academic Press, 600 p.

Tye, R.S., and Coleman, J.M., 1989, Depositional processes and stratigraphy of fluvially dominated lacustrine deltas: Mississippi Delta plain: Journal of Sedimentary Petrology, v. 59, no. 6, p. 973–996.

Uba, C.E., Heubeck, C., and Hulka, C., 2006, Evolution of the late Cenozoic Chaco foreland basin, southern Bolivia: Basin Research, v. 18, no. 2, p. 145–170, doi: 10.1111/j.1365-2117.2006.00291.x.

Van der Hammen, T., 1958, Estratigrafía del Terciario y Maestrichtiano continentales y tectogénesis de los Andes Colombianos: Boletín Geológico: Ingeominas Bogotá, v. 6, no. 1–3, p. 67–128.

Wagner, G.A., and Reimer, G.M., 1972, Fission track tectonics: The tectonic interpretation of fission track apatite ages: Earth and Planetary Science Letters, v. 14, no. 2, p. 263–268, doi: 10.1016/0012-821X(72)90018-0.

Wagner, G.A., and van den Haute, P., 1992, Fission-Track Dating: Dordrecht, Kluwer Academic Publishers, 285 p.

Waschbusch, P.J., and Royden, L.H., 1992, Episodicity in foredeep basins: Geology, v. 20, no. 10, p. 915–918, doi: 10.1130/0091-7613(1992)020<0915:EIFB>2.3.CO;2.

Watts, A.B., Karner, G.D., and Steckler, M.S., 1982, Lithospheric flexure and evolution of sedimentary basins: Philosophical Transactions of the Royal Society of London, Series A– Mathematical and Physical Sciences, v. 305, p. 249–281.

Wesselingh, F., Räsänen, M.E., Irion, G., Vonhof, H.B., Kaandorp, R., Renema, W., Romero-Pitman, L., and Gingras, M., 2002, Lake Pebas: A palaeoecological reconstruction of a Miocene long-lived lake complex in western Amazonia: Cainozoic Research, v. 1, no. 1–2, p. 35–81.

Manuscript Received 30 April 2007
Revised Manuscript Received 12 May 2008
Manuscript Accepted 6 July 2008

Printed in the USA